Journal of Crystal Growth 97 (1989) 497–501
North-Holland, Amsterdam

QUASI-EQUILIBRIUM CLUSTERING UPON SUPERSATURATION IN HOMOGENEOUS PHASE FORMATION

V.C. NONINSKI

Higher Institute of Chemical Technology, LEPGER, Sofia 1156, Bulgaria

Received 10 July 1988; manuscript received in final form 17 April 1989

The Gibbs–Thomson equation is observed while taking into account the size-dependence of the specific surface free energy, σ, derived in two different ways. It is shown that on supersaturation the most probable state of all atoms (molecules) in the parent phase in homogeneous phase formation is in the form of clusters and not of single atoms (molecules). Definition of critical supersaturation and barrierless condensation in the case of homogeneous phase formation is given.

1. Introduction

As is known in the theory of phase formation, the relation between the radius of the nucleus, r, and the supersaturation p_r/p_∞ is given by the Gibbs–Thomson isotherm:

$$RT \ln(p_r/p_\infty) = 2\sigma M/r\rho, \tag{1}$$

where R is the gas constant, T is the absolute temperature, M is the molecular weight of the substance, ρ is the density of the substance, p_r is the vapour pressure of the supersaturated system, p_∞ is the vapour pressure of the infinite drop (crystal) and σ is the specific surface free energy. Specific surface free energy of a cluster, σ, is the work for the formation of a unit of its surface. Usually, in eq. (1), σ is considered to be constant over the whole range of cluster dimensions. The constancy of σ is preserved for clusters of relatively high values of r. However, for clusters of smaller size the value of σ already becomes dependent on the radius of the drop. As shown by Gibbs [1], the dependence of σ on the surface curvature cannot be ignored when the problems of nucleation are treated, because the size of the nucleus is very small and the surface free energy begins to play a significant role in the work of formation of the cluster.

The first theoretical consideration of the effect of the droplet size on surface tension (specific surface free energy) is made by Tolman [2] on the basis of Gibbs's thermodynamic theory of capillarity and his own assessment of the sign and magnitude of the superficial density. Tolman derived the following equation for the said dependence:

$$\sigma = \sigma_\infty \exp\left[\int_\infty^{r_2} \frac{\frac{2\delta}{r_2^2}\left(1+\frac{\delta}{r_2}+\frac{\delta^2}{3r_2^2}\right)}{1+\frac{2\delta}{r_2}\left(1+\frac{\delta}{r_2}+\frac{\delta^2}{3r_2^2}\right)} \mathrm{d}r_2\right], \tag{2}$$

where r_2 is the cluster radius, δ is the half-interfacial thickness and σ_∞ is the specific surface free energy of the flat surface.

Later other authors also estimated the dependence of σ on the radius of the cluster [3–6]. The equations derived, however, contain empirical constants whose physical meaning is far from evident.

Noninski [7,8] derived an equation for the relation of σ upon r for convex and concave surface by calculating the energy of the Van der Waals interaction between a sphere and a medium of the same substance surrounding it:

$$\sigma = \frac{A}{d_0^2} + \frac{2A}{r^2}\ln\frac{d_0}{r+d_0}, \tag{3}$$

where

$$A = \tfrac{1}{15}\pi n^2 \beta,$$

0022-0248/89/$03.50

d_0 is the diameter of a molecule, n is the number of molecules in a unit volume, β is the constant from the expression for the energy of attraction between two molecules $E = -\beta/r_1^6$, r is the radius of the drop equal to the distance between the centre of the drop and the centres of the outmost, peripheral molecules, situated at the cluster/parent-phase interface.

As is seen, eq. (3) contains quantities which are known from the experiment or can be calculated with sufficient accuracy. Therefore, in the cases in which the experimental value of σ is known, eq. (3) can be checked. Proof for the validity of eq. (3) is the very good concordance between the calculated value of σ for flat surface of pure water (73.52 erg cm^{-2}) and the experimentally established value of σ for purified water (71.97 erg cm^{-2}). Other proof for the validity of the above can be found in ref. [8] where it is shown that r in (3) at $\sigma = 0$ should be equal to the distance between the centres of the molecules at the critical temperature (especially after considering the intermolecular Born repulsion forces). Indeed, the value of r calculated according to eq. (2) in ref. [8] at $\sigma = 0$ is confirmed by the literature experimental data for the distance between the molecules at the critical temperature of 52 substances given in table 1 of ref. [8].

In the present paper the Gibbs–Thomson equation is observed in which the dependence of σ upon the radius of the cluster is taken into account, according to an approximation of Tolman's formula (2) made in ref. [9]. The obtained curves are compared with the Gibbs–Thomson equation specified for $\sigma = f(r)$ in ref. [7].

2. Gibbs–Thomson equation for $\sigma = f(r)$ and $\sigma = f(r_2)$

If instead of σ = constant, the expression (3) is taken into account in the Gibbs–Thomson equation (1), the following equation is obtained for convex form of the drop (crystal) [7]:

$$p_r = p_\infty \exp\left[\frac{2AM}{RT\rho}\left(\frac{1}{rd_0^2} + \frac{2}{r^3}\ln\frac{d_0}{r+d_0}\right)\right]. \qquad (4)$$

On the other hand, eq. (2) gives another possibility to specify the Gibbs–Thomson equation (1) for the size dependence of σ. We shall use here the exponential approximation of Tolman's equation (2) made by Larson and Garside [9]:

$$\sigma = \sigma_\infty \exp(-2\delta/r_2), \qquad (5)$$

to obtain

$$p_{r_2} = p_\infty \exp\left[\frac{2M}{RT\rho}\frac{\sigma_\infty}{r_2}\exp\left(-\frac{2\delta}{r_2}\right)\right], \qquad (6)$$

where r_2 is the so-called radius of the particle bounded by the equimolar dividing surface and its value is determined by definition equations containing arbitrarily chosen constants [10].

In fig. 1 the Gibbs–Thomson isotherms for the formation of ice particles for σ = constant (according to eq. (1)), $\sigma = f(r)$ (according to eq. (4)) and $\sigma = f(r_2)$ (according to eq. (6)) are shown, the latter being plotted for 4 different values of δ. The curves in fig. 1 are obtained for $T = 270$ K, $d_0 = 2.76 \times 10^{-8}$ cm, $\sigma_\infty = 71.97$ erg cm^{-2}, $\rho = 0.999$ g cm^3, $A = 5.6008 \times 10^{-14}$ and $p_\infty = 8.1$ Torr. The value of the vapour pressure of ideal macrocrystal at 270 K and the value of the quantity A are calculated in ref. [7].

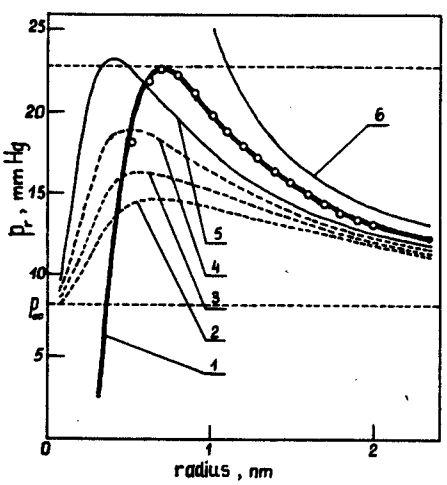

Fig. 1. Vapour pressure of ice particles, p_r, as a function of their radius. Curve 1 has been obtained according to eq. (4); (O) values calculated according to eq. (9) for $2\delta = 0.414$ nm). Curves 2, 3, 4 and 5 have been obtained according to eq. (6) for δ equal to 0.35, 0.30, 0.25 and 0.20 nm, respectively. Curve 6 has been obtained according to eq. (1) for σ = constant.

When observing the curves obtained according to eq. (4) (curve 1) and eq. (6) (curves 2–5), it is seen that all of them have a maximum, unlike curve 6 obtained according to eq. (1) in which σ = constant.

The values of δ and r_2 included in eq. (6) do not have a straightforward physical meaning and they are chosen arbitrarily. The physical meaning of the quantities included in eq. (4) is much more clear and eq. (4) can be used as a model for comparison when observing other models like the one expressed by eq. (6). As it can be seen from fig. 1, the form of the curve obtained according to eq. (6) that best of all approximates that obtained according to eq. (6) is attained at:

$$2\delta \approx 0.4 \text{ nm} \approx \tfrac{3}{2} d_0. \tag{7}$$

The obtained value of δ is more than an order of magnitude smaller than the value $\delta = 2.5$ nm accepted by Larson and Garside in ref. [9].

From fig. 1 is seen that if the difference in physical meaning of r_2 and r is taken into account the latter is of lower value than r_2 and is equal to

$$r \approx r_2 - 0.3 \text{ nm} \approx r_2 - 1.5\delta. \tag{8}$$

If we take into consideration the above, we can write instead of eq. (6):

$$p_r = p_\infty \exp\left[\frac{2M}{RT\rho}\frac{\sigma_\infty}{r_2 - 1.5\delta}\exp\left(-\frac{2\delta}{r_2 - 1.5\delta}\right)\right]. \tag{9}$$

In fig. 1 the points denoted by open circles represent the values obtained according to eq. (9). As is seen from fig. 1, the curve plotted according to eq. (9) coincides with that of eq. (4) for approximately $\delta/r < 0.5$. It is to be noted that the exponential approximation of eq. (2) made by Larson and Garside (eq. (6) in ref. [9]) holds for $\delta/r \ll 1$. We shall discuss here only the part of the curves where they coincide.

3. Discussion

Fig. 1 shows that at a given supersaturation, below that corresponding to the maximum of curve 1, two kinds of clusters exist. The clusters corresponding to the right-hand branch of the curve are in metastable equilibrium (critical clusters) – they will either grow up to a big crystal or will disperse upon a fluctuational respectively increase or decrease of their size. The cluster corresponding to the left-hand branch, however, will neither grow nor disperse upon accidental respectively increase or decrease of their size – these clusters are in a quasi-equilibrium state. This conclusion is made on the basis of two independently derived equations – eq. (4) and eq. (6) (respectively eq. (9)). As is known in the case of homogeneous condensation on ions, a maximum similar to that in curve 1 of fig. 1 is observed in refs. [41,42]. From the results in refs. [7,8] and those presented here, it follows that when taking into account the size dependence of σ, the maximum in the Gibbs–Thomson isotherm is observed in all the cases of homogeneous phase formation independent of whether the cluster is charged or not.

The size of these quasi-equilibrium clusters corresponds to tens of atoms (molecules) and will even be greater than the size observed in fig. 1, curve 1, should the forces of Born intermolecular repulsion, specific edge free energy, adsorbtion, etc. be taken into account. Therefore, statistical treatment is possible of this clustering and the laws of thermodynamics are applicable for its explanation.

We shall note here that clustering is observed experimentally upon supersaturation [14–34, 38–40] and even in saturated and undersaturated systems [35–37].

The critical supersaturation in homogeneous phase formation is usually defined as the supersaturation at which the rate of nuclei formation, I, defined by Volmer's equation [43],

$$I = A \exp(-W/kT), \tag{10}$$

is equal to unity, where I is the number of nuclei formed per unit of time in a unit volume and A is a kinetic factor determined by the transport of the substance from the parent phase to the nucleus. In practice this supersaturation is established by visual determining the appearance of the first cluster. Clearly, this subjective way of determination introduces uncertainty in the established value.

Instead of using eq. (1), another definition can be applied, similar to that in the case of homogeneous condensation on ions [42], heterogeneous phase formation at negative line tension, γ [11], and, as can be shown, also at $\gamma > 0$, i.e. the critical supersaturation in homogeneous phase formation is the supersaturation corresponding to the maximum in curve 1 in fig. 1. In terms of ref. [42], above the critical supersaturation the homogeneous phase formation is already a barrierless process. At these supersaturations the rate-determining step of the phase formation is the transport of substance from the parent phase to the cluster and the kinetic obstacles are eliminated. The latter can be understood if it is remembered that in terms of ref. [42], the barrier that should be overcome to form a nucleus at a given supersaturation is equal to the difference between the work for the formation of the critical cluster and the work for the formation of the quasi-equilibrium one. At the maximum of curve 1 of fig. 1, this work is zero.

When observing curve 1 in fig. 1 it can be seen that the conclusions in refs. [9,10] regarding clustering upon supersaturation can be extended. As it can be seen when analysing curve 1 in fig. 1, the most probable state of all atoms (molecules) in a supersaturated system in homogeneous phase formation is in the form of clusters and not of separate, single atoms (molecules). We shall only note here that this conclusion holds also for heterogeneous phase formation. Furthermore, this conclusion does not apply only for a limited region, but applies also for the whole region of supersaturations, at least where kinetic and not transport phenomena are rate-determining. The size of the quasi-equilibrium clusters is dependent on the supersaturation and a certain size of these clusters (in the above limits) corresponds to every supersaturation.

Clearly, the above conclusions should influence the derivation of the kinetic equations of phase formation since it is more probable that the elementary building particle at every supersaturation is a cluster of atoms (molecules) rather than a single, separate atom (molecule). This will lead to a somewhat "quantum" treatment of nucleation and growth with "allowed" and "forbidden" cluster sizes depending on the supersaturation. This question shall be treated in future communications.

References

[1] J.W. Gibbs, Collected Works, Vol. 1 (Longmans–Green, London, 1928) p. 219.
[2] R.C. Tolman, J. Chem. Phys. 17 (1949) 333.
[3] J.K. Lee, F.F. Abraham and G.M. Pound, Surface Sci. 34 (1973) 745.
[4] C.L. Briant and J.J. Burton, J. Chem. Phys. 63 (1975) 2045.
[5] K. Nishioka, Phys. Rev. A16 (1977) 2143.
[6] D.H. Ramussen, M. Sivaramakrishnan and G.L. Leedom, AIChE Symp. Ser. No. 125, 78 (1982) 1.
[7] C.I. Noninski, Khimia i Industria (Bulgaria) 33 (1961) 144.
[8] C.I. Noninski, Khimia i Industria (Bulgaria) 39 (1967) 208.
[9] M.A. Larson and J. Garside, J. Crystal Growth 76 (1986) 88.
[10] O. Söhnel and J. Garside, J. Crystal Growth 89 (1988) 202.
[11] A. Scheludko, Colloids Surfaces 7 (1983) 81.
[12] Spravochnik Khimika, Vol. 1 (Goskhimizdat, Leningrad, 1951) pp. 858, 880.
[13] Ya.K. Sirkin and M.E. Dyatkina, Chemical Bond and Structure of the Molecules (Goskhimizdat, Moscow, 1946) p. 317 (in Russian).
[14] E. Pozner, Zh. Fiz. Khim. 13 (1939) 889.
[15] Ya. I. Frenkel, Kinetic Theory of Liquids (Akad. Nauk SSSR, Moscow, 1945) (in Russian).
[16] M.V. Tovbin and S.N. Krasnova, Zh. Fiz. Khim. 25 (1951) 161.
[17] L.N. Matusevich and K.N. Shabalin, Zh. Prikl. Khim. 25 (1952) 1157.
[18] J.P. Borel, Helv. Phys. Acta 27 (1954) 485.
[19] M.V. Tovbin and S.N. Krasnova, Zh. Fiz. Khim. 21 (1951) 32.
[20] V.G. Khlopin, Selected Papers, Vol. 1 (Akad. Nauk SSSR, Moscow, 1957) (in Russian).
[21] M.V. Tovbin and O.V. Savinova, Nauk. Zap., Kiev Univ. 16 (1957) 45.
[22] N.M. Fletcher, Sci. Progr. 54 (1966) 227.
[23] L.N. Matusevich, Crystallization from Solutions in the Chemical Industry (Khimiya, Moscow, 1968) (in Russian).
[24] A.A. Chernov, Vestn. Akad. Nauk SSSR 11 (1968) 60.
[25] J.W. Mullin and C.L. Leci, Phil. Mag. 19 (1969) 1075.
[26] Yu.A. Serebryakov and E.V. Khamskii, Kristallografia 15 (1970) 1226.
[27] A.T. Allen, M.P. McDonald, W.M. Nicol and R.M. Wood, Nature 235 (1972) 36.
[28] A.T. Allen, M.P. McDonald, W.M. Nicol and R.M. Wood,

in: Particle Growth in Suspensions, Ed. A.L. Smith (Academic Press, London, 1973) p. 239.
[29] D.M. Rasmussen and A.P. MacKenzie, J. Chem. Phys. 59 (1973) 5003.
[30] J. Dousma and P.L. de Bruyn, J. Colloid Interface Sci. 56 (1976) 527.
[31] R.J,. Stol, A.K. van Helden and P.L. de Bruyn, J. Colloid Interface Sci. 57 (1976) 115.
[32] R.M. Heist, K.M. Colling and C.S. DuBuis, J. Chem. Phys. 65 (1976) 5147.
[33] Y.G. Russel and R.M. Heist, J. Chem. Phys. 69 (1978) 3723.
[34] G. Agarwall and R.M. Heist, J. Chem. Phys. 73 (1980) 902.
[35] G.A. Hussmann, M.A. Larson and K.A. Berglund, in: Industrial Crystallization '84, Eds. S.J. Jančić and E.J. de Jong (Elsevier, Amsterdam, 1984) p. 21.
[36] P.M. McMahon, K.A. Berglund and M.A. Larson, in: Industrial Crystallization '84, Eds. S.J. Jančić and E.J. de Jong (Elsevier, Amsterdam, 1985) p. 229.
[37] M. Nicolas and P. Joyes, Surface Sci. 156 (1985) 189.
[38] M.A. Larson and J. Garside, J. Chem. Eng. Sci. 41 (1986) 1285.
[39] Y.C. Chang and A.S. Myerson, AIChE J. 33 (1987) 697.
[40] T. Stace, Nature 327 (1987) 186.
[41] J.J. Thomson, Electrizitätdurchgang in Gasen (Teubner, Leipzig, 1901) p. 148.
[42] G. Tomford and M. Volmer, Ann. Physik (Leipzig) 33 (1938) 109.
[43] M. Volmer, Kinetic der Phasenbildung (Steinkopf, Dresden, 1939).

Small Stable Drops and Crystals in Supersaturated Homogeneous and Heterogeneous Systems at Positive Specific Linear Free Energy

VESSELIN CHRISTOV NONINSKI

Laboratory for Electrochemistry of Renewed Electrode–Solution Interface (LEPGER), P.O. Box 9, Sofia 1504, Bulgaria

Received September 30, 1988; accepted October 5, 1990

Existence during supersaturation of quasi-equilibrium clusters of atoms (molecules), conditionally called small stable drops and crystals, in homogeneous and heterogeneous phase formation is discussed. It is shown that these small stable drops can exist not only when the specific linear free energy (specific edge free energy λ, respectively line tension γ_l, is negative but also in cases when λ and γ_l are positive. It is shown that small stable drops always exist when homogeneous and heterogeneous phase formation is thermodynamically possible; the sign of the line tension does not determine the possibility that a small stable drop can exist.

Nowadays theoretical methods employing radial distribution and correlation functions are widely applied in the classical theory of capillarity (1, 2). There is another approach to this question which was foreseen by Tolman (3): "Indeed it will ultimately seem more satisfactory to continue the investigation using the concept of forces exerted by individual molecules and the more detailed methods of molecular mechanics." Using a similar approach Noninski (4, 5) was able to derive an equation for the size dependence of the specific surface free energy σ. This size dependence is important to take into account especially when observing small drops (crystals); ignoring the size dependence of σ will lead to incorrect conclusions when treating, e.g., questions of nucleation. The σ values calculated from the equation derived in Ref. (4) for different substances are in excellent concordance with experimental values. Further, it was observed (4, 5) that when the specific surface free energy in the Gibbs–Thomson isotherm is considered size dependent, which is the real case, the isotherm changes its form and far-reaching, so far unknown, conclusions can be drawn. For instance, it has been found (4, 5), that when such specified Gibbs–Thomson isotherms referring to convex and concave forms are juxtaposed, a drop (cluster) of atoms (molecules) is the thermodynamically stable formation (at zero supersaturation). Thus, at equilibrium, an ideally built structure of the crystal is hardly possible. Further specification of the Gibbs–Thomson isotherm in some cases of phase transformations, which should not be ignored when small drops (crystals) are treated, can be done also by considering the effect of the specific line free energy (slfe) (4–11).

In the present paper another type of cluster is discussed whose existence follows from the specified Gibbs–Thomson isotherm upon supersaturation. These are quasi-equilibrium formations but for simplicity here they conditionally are called small stable drops. These quasi-equilibrium clusters are not the critical nuclei of a new phase.

Another aim of the present paper is to answer the question whether quasi-equilibrium clusters (small stable drops) can exist not only at negative but also at positive slfe. For homogeneous phase formation this question has not been treated so far, while in the case of heterogeneous phase formation the existence

0021-9797/91 $3.00

of quasi-equilibrium small stable drops upon supersaturation was found by Scheludko *et al.* (6–11) only for the case of negative slfe (line tension, γ_1).

THEORY

Homogeneous Phase Formation

For the case of homogeneous phase formation the conclusions here will be based on an equation for the relationship between the specific surface free energy σ and the radius of the drop (crystal) r and the Gibbs–Thomson isotherm specified for this size-dependent σ. Derivation of this equation was carried out by Noninski (4, 5) when calculating the energy of the van der Waals interaction between a sphere and the medium of the same substance surrounding it.

Previous papers (4, 5) were published in Bulgarian; therefore, in the present paper the derivation of $\sigma = f(r)$ in Ref. (4) is outlined briefly. Here we summarize only the derivation of $\sigma = f(r)$ for a convex surface and leave for the future the discussion of the other important conclusions in Refs. (4, 5), such as the proof for the existence of a thermodynamically stable drop, the size of that drop, the influence of the above on crystal growth, and interpretation of the critical temperature of the substance.

The dependence of σ on r is derived in Ref. (4) in the following way: For simplicity the surface whose σ is to be determined is considered to be spherical. The problem in calculating σ of a sphere is reduced to the calculation of the potential energy of interaction between the sphere and the remaining (nonspherical) part of the body from which the sphere is imaginatively obtained at a moment before its tearing from the remaining (nonspherical) part. The work for reversible isothermic tearing and moving apart, up to infinity, of the parts of a body is equal to the absolute value of the potential energy of interaction between the same parts before their tearing.

The energy of interaction between two molecules is given by the expression

$$E' = -\frac{\beta}{r_1^6} + \frac{\gamma}{r_1^q} \qquad [1]$$

where β, γ, and $q > 6$ are constants, and r_1 is the distance between the centers of the molecules. The first term in Eq. [1] expresses the energy of the van der Waals attraction and the second term, the energy of Born intermolecular repulsion.

It should also be pointed out here that when the molecules of the remaining (nonspherical) part of the body are moving apart in a radial direction from the spherical part they are also moving apart from each other. Keeping in mind the latter it can easily be understood that only one surface is being obtained when the described tearing takes place, namely, the surface of the spherical drop (crystal). The work for moving apart from each other, up to infinity, of the molecules of the nonspherical part of the body has nothing in common with the work for overcoming the attraction between the sphere and the molecules that are being moved apart from it. It is the latter work that determines σ.

When solving the above problem not only the magnitude of the dispersion, the orientation, and the induction van der Waals forces of interaction between the two molecules are taken into account, but also the directions of the interaction between each molecule of the body and all the molecules of the other body are considered.

As a result and after solving some problems of a mathematical nature an equation is derived for the energy of interaction between one molecule of the spherical drop (crystal) with one molecule of the medium surrounding it (for simplicity the Born repulsion forces are neglected; such neglect is physically consistent because the repulsion forces act at a very close distance and disappear with distance much faster than the forces of attraction). This equation is integrated so that the energy of

interaction between one molecule in the spherical part of the body with all the molecules of the remaining (nonspherical) part is obtained. Then the expression obtained is integrated again for all the molecules in the spherical part of the body. Thus, the energy of attraction between the two parts of the body, spherical and nonspherical, U, is found. Now that the equation for U is known it is noted in Ref. (4) that this energy corresponds to that at the closest distance at which the body's molecules can contact each other, i.e., the distance between the centers of the separate molecules, which virtually is equal to their diameter, d_0. The work for overcoming the forces of attraction when moving the nonspherical part of the body apart from the spherical one at a distance from d_0 up to ∞ is equal to $-U$. Since in the course of this moving apart, a new surface, O, is created, of the size $O = 4\pi r^2$, the work for the creation of a unit surface which virtually is the specific surface free energy will be

$$\sigma = -\frac{U}{4\pi r^2}. \qquad [2]$$

When the expression for U derived above is substituted in Eq. [2] one obtains

$$\sigma = \frac{A}{d_0^2} + \frac{2A}{r^2} \ln \frac{d_0}{r+d_0} \qquad [3]$$

where

$$A = \tfrac{1}{15}\pi n^2 \beta$$

and d_0 is the diameter of a molecule, n is the number of molecules in a unit volume, β is the constant from the expression for the energy of attraction between two molecules, $E = -\beta/r_1^6$, r is the radius of the drop equal to the distance between the center of the drop and the centers of the outmost, peripheral molecules, situated at the cluster/parent phase interface.

As is seen, Eq. [3] contains quantities which are known from the experiment or can be calculated with sufficient accuracy. Therefore, in the cases in which the experimental value of σ is known Eq. [3] can be checked. A proof for the validity of Eq. [3] is the very good concordance between the calculated value of σ for a flat surface of pure water (73.52 erg cm^{-2}) and the experimentally established value of σ for purified water (71.97 erg cm^{-2}) (13).

While in the case of water all the three types of intermolecular interaction forces—orientation, induction, and dispersion—are available, there are simple kinds of molecules like Ar, H_2, and N_2 whose only intermolecular force of interaction is dispersion. In this case, instead of β the constant B from the Lennard-Jones (LJ) equation can be used. In Table I, just as an illustration, experimental σ values for various simple molecules are presented together with σ values calculated by the equation

$$\sigma = \frac{\pi n^2 B}{15 d_0^2} \qquad [4]$$

obtained from Eq. [3] for a flat surface and for $\beta = B$, where the B values are calculated from the virial coefficients [method of Lennard-Jones (12, p. 293)]. The other values of the constants used for these calculations are from Refs. (1, 12–14). Clearly, the result will depend strongly on the accuracy of calculation of constant B.

Taking into account Eq. [3] the Gibbs–Thomson equations are obtained for convex and concave forms, respectively, specified for $\sigma = f(r)$ (4, 5):

TABLE I

Molecule	σ (dyn/cm) Calculated	σ (dyn/cm) Experimental
Ar	11.4 (87.3 K)[a]	12.67 (87 K)
H_2	2.01 (20.2 K)	1.98 (19.9 K)
N_2	8.68 (77.2 K)	8.29 (80 K)

[a] Corresponding temperatures in parentheses.

$$\ln \frac{p_r}{p_\infty} = \frac{2AM}{RT\rho}\left(\frac{1}{rd_0^2} + \frac{2}{r^3} \cdot \ln \frac{d_0}{r + d_0}\right) \quad [5]$$

$$\ln \frac{p_{r_0}}{p_\infty} = -\frac{2AM}{RT\rho}\left(\frac{1}{r_0 d_0^2} + \frac{2}{r_0^3} \cdot \ln \frac{d_0}{r_0 + d_0}\right). \quad [6]$$

Here, T is the absolute temperature, M is the molecular weight, R is the gas constant, ρ is the density of the substance, p_r is the vapor pressure of small drops (crystals), p_∞ is the vapor pressure of the infinite drop (infinite crystal), and r_0 is the radius of the concave form. Equation [5] has a maximum and Eq. [6] has a minimum.

It was proved (4, 5) that a thermodynamically stable drop of finite size exists (having $\sigma = 0$). It was shown that the size of this thermodynamically stable drop for every substance does not depend on the nature of the intermolecular forces and is determined solely by the size of that substance's molecules. It was also shown that the volume of the thermodynamically stable drop (especially when Born forces of intermolecular repulsion, specific edge free energy, etc., are taken into account) is about 64 times greater than the volume of a single molecule. In such a volume tens of molecules are contained (approximately one and the same number for different substances). Therefore, the thermodynamically stable drop (crystal) is a particle of relatively significant dimensions for which the laws of statistics hold; therefore, the thermodynamics laws can be applied when observing it. This thermodynamically stable drop can be looked upon as an entirely differentiated entity of the new phase with a clearly delineated interface and with dimensions of the order of those of highly disperse colloid particles. These clusters are equally stable with the ideally built macrocrystal and can aggregate as building particles of a macrocrystal having a disperse structure. This disperse structure macrocrystal has inner surfaces whose vapor pressure is lower than that of the ideally built macrocrystal, and condensation will take place on that disperse structure crystal. The condensation continues until the entire ideal macrocrystal disappears.

Another proof for the validity of the above theory can be found in Ref. (5) where it is shown that the radius of the thermodynamically stable drop in Eq. [3] at $\sigma = 0$ should be equal to the value of the distance between the centers of the molecules at the critical temperature (especially after considering the intermolecular Born repulsion forces). Indeed, the value of r calculated according to Eq. [2] in Ref. (5) at $\sigma = 0$ is confirmed by the literature experimental data for the distance between the molecules at the critical temperature for 52 substances given in Table I of Ref. (5).

It should be noted here that in Refs. (4, 5) the conclusions are based on well-defined and physically clear presumptions, avoiding the use of arbitrary (conditional) notions, like Gibbs dividing surface or surface of tension. For instance, the diameter of a molecule, a basic parameter in Eq. [3], has a clear physical meaning, whereas the distance between the surface of tension and the surface of zero adsorption is an arbitrarily chosen quantity [cf. (1, pp. 31, 32)]. How the position of the dividing surface is chosen can be seen, e.g., in Ref. (15). As it concerns the physical meaning of LJ distance, the latter, since a result of an approximation, is also not too clear physically compared to the well-defined quantity "diameter of an atom."

We would like also to note that the correction term $\partial\sigma/\partial r$ in Refs. (16, 17) is also connected with the arbitrariness in choice of the dividing surface. As seen in Ref. (1, p. 33) the surface of tension, where the Gibbs–Thomson equation holds in its simplest form, is defined as a surface where the term $\partial\sigma/\partial r$ is equal to zero.

It is interesting to note that in the case of simple molecules, Eq. [4] is quite similar to the known equation (keeping the present notation)

$$\sigma = \frac{2\pi Bn^2}{(m-2)(m-3)(m-4)d_0^{m-4}} \times \left[1 - \frac{(m-4)}{(n-4)}\right]$$

which for $m = 6$ and $n = 9$ obtains the form (12, p. 850)

$$\sigma = \frac{\pi n^2 B}{20 d_0^2}.$$

In some cases of homogeneous phase formation (e.g., ice crystal/water vapor) the quantity specific linear (edge) free energy λ can also play a significant role, especially at sufficiently small crystals, although the λ value is much less than σ. As is known in this case, the Gibbs–Thomson equation for a crystal (drop) taking into account λ has the form (4)

$$p_r = p_\infty \exp\left[\frac{2AM}{RT\rho}\left(\frac{1}{rd_0^2} + \frac{2}{r^3}\ln\frac{d_0}{r+d_0}\right)\right] \times \exp\frac{\lambda}{r^2}. \quad [7]$$

The quantity λ can be both positive and negative because both concave and convex forms can be thought.

In Fig. 1 the vapor pressure of ice particles, p_r, is plotted as a function of their radius, r, according to Eq. [7] for $\lambda = 0$, $\lambda = -2 \times 10^{-15}$, and $\lambda = 2 \times 10^{-15}$ dyn and for $T = 270$ K, $\rho = 0.999$ g cm^{-3}, $d_0 = 2.76 \times 10^{-8}$ cm, $A = 5.6008 \times 10^{-14}$ [according to Ref. (4)], $M = 18$, $\sigma_\infty = 71.97$ erg cm^{-2}, and $p_\infty = 8.1$ mmHg. The value of the vapor pressure of the ideal macrocrystal at 270 K is calculated in Ref. (4). The value of the quantity A is calculated in Ref. (4) in the following way: It is taken into account that in the van der Waals forces the orientation effect (the effect of Keesom) plays the greatest role—it constitutes 77% of the forces (14). The energy of the orientation effect, E_{0r}, is given by the expression

$$E_{0r} = -\frac{2}{3}\frac{\mu^4}{r_1^6 kT} = \frac{\beta_{0r}}{r_1^6} \quad [8]$$

where μ is the dipole moment of the molecules (for water molecules $\mu_{H_2O} = 1.84 \times 10^{-18}$ esu cm (1.84 D) (13)), $k = 1.38 \times 10^{-16}$ erg K^{-1} is the Boltzmann constant, $T = 298.2$ K. Therefore, the full energy of the van der Waals interaction is

$$E = -\frac{\beta_{0r}}{0.77 r_1^6} = -\frac{\beta}{r_1^6} = -\frac{2.4116 \times 10^{-58}}{r_1^6}.$$

From this equation $\beta = 2.4116 \times 10^{-58}$; the number of water molecules in 1 cm^3 is $n = N/18.1 = 3.33 \times 10^{22}$. Therefore, $A = \frac{1}{15}\pi n^2 \beta = 5.6008 \times 10^{-14}$.

As is seen in Fig. 1 the specified Gibbs–Thomson isotherm determines the fact that upon supersaturation, even in the case of uncharged particles, two types of cluster (drops, crystals) always exist in the system. The first type is in unstable equilibrium. This cluster is known as the critical nucleus. The other type of cluster is in metastable equilibrium; this is the quasi-equilibrium cluster, conditionally called by us small stable drops. Therefore, the conclusion can be drawn that during supersaturation the most probable state of the atoms (molecules) is that of clusters and not of separate single atoms (molecules).

Figure 1 shows that with a negative value of λ, an increase in the radius of the small stable drop is observed. The region of r values in which small stable drops can exist also increases with the negative λ value, the maximum of the curve $p_r = f(r)$ decreasing at that. In the case of $\lambda > 0$ the opposite is observed;

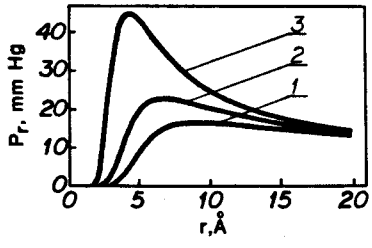

FIG. 1. Vapor pressure of small ice particles, p_r, as a function of their radius, r. (1) $\lambda = -2 \times 10^{-15}$ dyn, (2) $\lambda = 0$ dyn, (3) $\lambda = 2 \times 10^{-15}$ dyn.

with positive λ, decreases both in radius of the small stable drop and in the region where small stable drops can exist are observed, the maximum increasing at that. The latter changes are much more expressed than in the case of $\lambda < 0$. Figure 1 shows only the principal possibility for the existence of stable particles both when λ is positive and when λ is negative. Discussion of the real order of λ values is beyond the scope of this paper.

A basic conclusion can also be made from the above that in the case of homogeneous phase formation, the possibility of the existence of small stable drops is not determined by the sign of the specific edge free energy; whenever λ takes part in the phase formation small stable drops can exist both with positive and with negative λ.

Another important conclusion that can be drawn from the Gibbs–Thomson equation specified for $\sigma = f(r)$ is that critical supersaturation for homogeneous phase formation can be defined as

$$kT \ln(p/p_\infty) = \frac{2\sigma v}{r}$$

where v is the molecular volume and k is the Boltzmann constant. The following equation is obtained:

$$\ln(p/p_\infty) = \frac{2v\sigma^2}{kT\gamma_t}(\cos\Theta_\infty - \cos\Theta)\sin\Theta.$$

The values of n in Ref. (10) are obtained by expressing r from Eq. [9] and inserting it in the equation for the volume, V, of a segment of a sphere,

$$V = \frac{\pi}{3} r^3(2 - 3\cos\Theta + \cos^3\Theta),$$

and dividing by the volume of one molecule:

$$n = \frac{\pi}{3v} \cdot \frac{\gamma_t}{\sigma^3} \cdot \frac{2 - 3\cos\Theta + \cos^3\Theta}{(\cos\Theta_\infty - \cos\Theta)^3 \sin^3\Theta}.$$

In Fig. 2 the dependence of $\ln(p/p_\infty)$ versus n for water is shown as obtained in the above way for a reasonable value of $\gamma_t = 1 \times 10^{-5}$ dyn and $\sigma = 72$ dyn cm^{-1}, $\Theta_\infty = 45°$, $kT = 4 \times 10^{-14}$ erg, $v = 2.93 \times 10^{-23}$ cm^3.

One can note that unlike the first part of this paper, here, in the case of heterogeneous phase formation, we consider the specific surface free energy σ as size independent, only γ_t being considered size dependent through Eq. [9]. We apply this simplification here since it turned out that in the case of heterogeneous phase formation the $\sigma = f(r)$ dependence does not influence, in principle, the main conclusions drawn here. The effect of the $\sigma = f(r)$ dependence in the case of heterogeneous phase formation will be discussed in future communications.

Let us especially note that Fig. 2 is a more detailed presentation of the upper part of Fig. 1 in Ref. (9). This more detailed presentation leads to conclusions to be discussed now, which were unnoticed by the author of Ref. (9).

From Fig. 2 it is seen that at a given supersaturation in the region of approx $0.789 < \ln(p/p_\infty) < 0.797$ a drop exists of a given dimension (radius, r, or number of atoms, n) related with the left-hand branch, AB, of the curve ABC which will neither augment nor disappear upon an accidental increase in its dimensions. This drop will remain stable and it will represent the most probable dimension of the clusters for a given supersaturation. For clarity in Fig. 2, only the part of the whole curve corresponding to $110° < \Theta < 130°$ is represented; the slope of the two branches of

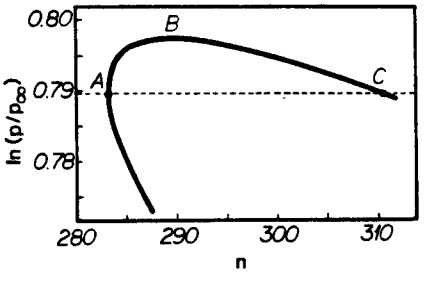

FIG. 2. Logarithm of supersaturation, $\ln(p/p_\infty)$, as a function of the number of atoms in the drop, n. See details in the text.

the curve outside these limits continues to be negative (i.e., corresponding to unstable drops) for the part of the curve below the broken line (corresponding to $\Theta < 118°$).

An important fact, also unnoticed in Ref. (9), is that according to Ref. (9, Fig. 1) at $\gamma > 0$ there are small drops of certain Θ values the existence of which is thermodynamically impossible. For instance, according to Ref. (9, Fig. 1) at a given supersaturation, unstable drops of two different dimensions exist or for a given dimension of the drop there are two differing values of the supersaturation (resp. vapor pressure). This is an evidently impossible situation: if in a closed system there are two bodies of different vapor pressures, the body with the lower vapor pressure will be thermodynamically more stable. Thus when equilibrium is reached the body with the higher vapor pressure should disappear, its vapors being condensed on the body with the lower vapor pressure. Therefore, when thermodynamic equilibrium is reached a body characterized with a single value of vapor pressure will remain in the system. These considerations lead us to the indisputable conclusion that from a thermodynamic point of view, it is impossible for the curve containing points A, B, and C (curve 1) and the curve below point A (curve 2) to exist simultaneously. Only one of these curves can exist in reality and the question is which one.

This question can be solved unambiguously only through experiments. Unfortunately, no experimental results are available so far. Nevertheless, we shall try to make some discussion and draw conclusions by applying analogy.

It is seen that in the case of $k < 0$ shown in Ref. (9, Fig. 2), a curve with a maximum is observed. In the case of homogeneous phase formation a maximum is obtained in the plot of $\ln(p/p_\infty)$ versus drop radius and according to Ref. (4, Eq. [16]) taking into account $\sigma = f(r)$ dependence, for both negative and positive specific edge free energy λ. Note that the quantity λ corresponds to k. It should especially be noted again, as was done above, that the derivations in Ref. (4) are based on quantities having strictly defined and clear physical meaning.

Proceeding from the above analogy it can be concluded that curve 1 is the physically possible one and curve 2, which is only a result of the mathematical calculations, should be ignored.

According to curve 1 in Fig. 2 only the drops having contact angle values of approx $\Theta > 118°$ (to the right of point A) can thermodynamically exist. However, we note further that in Ref. (9, Fig. 2) and in the case of homogeneous phase formation (4) there is no breaking of the curves at a point similar to point A. In Fig. 1 no curve to the left of point A is observed, probably because of some inaccuracy of the equations used to obtain the curve in Ref. (9, Fig. 2). This question, however, is beyond the scope of the present paper.

In the case of $\gamma_t > 0$ critical supersaturation can also be defined as is done in Ref. (9) for the case of $\gamma_t < 0$. In Fig. 2 point B defines the critical supersaturation for the case of $\gamma_t > 0$.

From the above it can be concluded that unlike the statements in Refs. (6–11), during heterogeneous phase formation small stable drops can exist not only when $\gamma_t < 0$ but also in cases when $\gamma_t > 0$ for $\Theta > \Theta_\infty$, the latter cases being the only possible ones when $\gamma_t > 0$.

Therefore, the possibility of the existence of small stable drops in phase formation is determined only by thermodynamic criteria. Other criteria, such as the sign of the slfe, cannot be decisive. The sign of the slfe can influence only the direction of the changes and the kinetic parameters of the process of phase formation.

REFERENCES

1. Ono, S., and Kondo, S., "Molecular Theory of Surface Tension in Liquids." Izdatel'stvo Inostrannoi Literaturi, Moscow, 1963. [in Russian]
2. Rowlinson, J. S., and Widom, B., "Molecular Theory of Capillarity." University Press, Oxford, 1982.
3. Tolman, R., *J. Chem. Phys.* **17**, (1949).
4. Noninski, C. I., *Khim. Ind. (Bulg.)*, No. 5, **33**, 144 (1961).
5. Noninski, C. I., *Khim. Ind. (Bulg.)*, No. 5, **39**, 208 (1967).

6. Scheludko, A., Toshev, B., and Platikanov, D., *in* "Modern Theory of Capillarity," pp. 163–182. Akademie Verlag, Berlin, 1981; *Ann. Univ. Sofia Fac. Chem.* **71**(1), 111 (1976/1977).
7. Scheludko, A., Chakarov, V., and Toshev, B., *J. Colloid Interface Sci.* **82**, 83 (1981).
8. Scheludko, A., *Colloids Surf.* **1**, 191 (1980).
9. Scheludko, A., *Colloids Surf.* **7**, 81 (1983).
10. Scheludko, A., Toshev, B., and Platikanov, D., "31st IUPAC Congress, Sofia (1987), Proceedings, p. 180.
11. Toshev, B. V., Platikanov, D., and Scheludko, A., *Langmuir* **4**, 489 (1988).
12. Moelwyn-Hughes, E. A., "Physical Chemistry." Izdatel'stvo Inostrannoi literaturi, Moscow, 1962. [in Russian]
13. "Short Handbook of Chemistry" [in Russian], Naukova Dumka, Kiev, 1974; "Handbook of Chemistry and Physics," 31st ed. (C. D. Hodgman, Ed.), p. 1747, Chemical Rubber Co., Cleveland, OH, 1949.
14. "Short Handbook of Chemistry." Izdatel'stvo Akademii Nauk Ukrainskoi SSR, Kiev, 1963. [in Russian]
15. Söhnel, O., and Garside, J., *J. Cryst. Growth* **89**, 202 (1988).
16. Shcherbakov, L. M., *Trudi Tul'skogo Mekhan. Inst.* **7**, 117 (1955).
17. Shcherbakov, L. M., *Koloid. Zh. (USSR)* **20**, 759 (1958).
18. Gibbs, J. W., "The Scientific Papers of J. Willard Gibbs," Vol. 1, "Thermodynamics," p. 288. Dover, New York, 1961.
19. Gretz, R. D., *J. Chem. Phys.* **45**, 3160 (1966).
20. Wesselovskii, V. S., and Pertzev, V. N., *Zh. Fiz. Khim. (USSR)* **8**, 245 (1936).

Colloids and Surfaces, 42 (1989) 205-207
Elsevier Science Publishers B.V., Amsterdam — Printed in The Netherlands

Brief Note

Stable Drop at Positive Line Tension

V.C. NONINSKI

Higher Institute of Chemical Technology, Lepger, Sofia 1156 (Bulgaria)

(Received 29 March 1988; accepted 20 June 1989)

ABSTRACT

In the present note it is shown that on supersaturation stable drops can, in principle, exist not only when the line tension, k, is negative but also in cases when $k>0$. Furthermore, it is pointed out that the decisive criteria for the existence of stable drops are thermodynamic ones, and not the sign of the line tension.

This note deals with the dependence of the logarithm of the supersaturation, $\ln(p/p_\infty)$, (where p is the vapour pressure of a small liquid drop and p_∞ is the vapour pressure of an infinite drop) as a function of the number of atoms in the liquid drop (in the case of heterogeneous phase formation), n, when the line tension [1,2] $k>0$ and the contact angle between droplet and substrate, θ, is greater than the contact angle of the large drop (for which the radius of the wetting perimeter $r\to\infty$), θ_∞.

We shall consider the case of the electrochemical deposition of mercury treated in Ref. [3], although the same conclusions also apply for other cases of heterogeneous phase formation. In Ref. [3], instead of the dependence $\ln(p/p_\infty)$ versus n the dimensionless quantity

$$\tilde{K}=(\cos\theta_\infty-\cos\theta)\sin\theta$$

versus the linear size of the drop in a dimensionless form

$$\tilde{l}=\frac{\sigma}{k}\left[\frac{3V}{\pi}\right]^{1/3}$$

is used (where σ is the surface tension and V is the volume of the drop). This exchange of the $\ln(p/p_\infty)$ versus n dependence by $\tilde{K}$ versus $\tilde{l}$ is possible because, as has been shown in Ref. [3] "the dependence $\tilde{K}$ versus $\tilde{l}$ reflects the changes in vapour pressure (supersaturation) with the change in drop size". As is claimed in Ref. [3] for the above conditions, namely $k>0$ and $\theta>\theta_\infty$, two curves of negative slope exist (Fig. 1 in Ref. [3]), so that "the states de-

0166-6622/89/$03.50

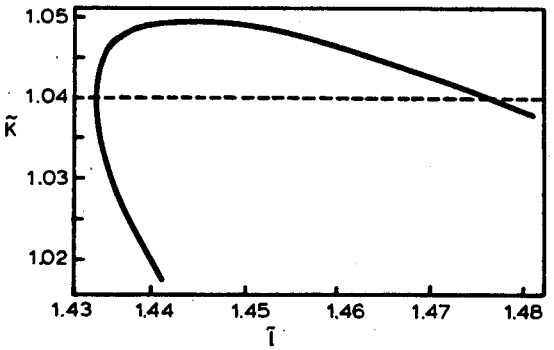

Fig. 1. Variation of $\tilde{K}$ with $\tilde{l}$ (see text) for $\Theta_\infty = 45°$, $k = 3.9 \cdot 10^{-5}$ dyn.

scribed by them are unstable: by an accidental enlargement of the equilibrium drop size its vapour pressure will diminish and the drop will continue to grow".

However, when the region of higher values of $\tilde{K}$ in Fig. 1 of Ref. [3] is observed it is seen that at a given Θ_∞ the branch of the curve with lower $\tilde{l}$ has a positive slope. This fact, unnoticed by the author of Ref. [3], can be seen in the curve presented in Fig. 1 above the broken line. This figure is obtained using the values of the constants given in Ref. [3] for a reasonable positive value of $k = 3.9 \cdot 10^{-5}$ dyn. It is necessary to note here that, because so far we are unaware of the real value of $k > 0$, if any, in the case of Hg electrodeposition, and also because the curve in Fig. 1 is plotted upon acceptance of $\sigma = \text{const}$ (note that $\sigma = \text{const}$ is accepted not only in the Gibbs–Thomson equation but also in the equation for k), which virtually does not hold for small drops, the conclusions from the figure can be drawn, for now, only in principle, utilizing only its form. In fact the conclusions from Fig. 1 in Ref. [3] were also drawn in principle because of the reasons stated above.

From Fig. 1 is seen that, above the broken line, a region of supersaturations exists where two forms of the new phase are in equilibrium: one is stable and the other unstable. The fact that such a region (although small) exists runs contrary to the claim in Refs [3–7] that a stable drop of the new phase is possible only when $k < 0$, and proves that stable drops can also exist in the case of a positive line tension ($k > 0$). Figure 1 also shows that the definition of critical supersaturation in terms of Refs [3 and 7] can be applied not only when $k < 0$ but also when $k > 0$.

REFERENCES

1 J.W. Gibbs, The Scientific Papers of J. Willard Gibbs, Vol. 1, Thermodynamics, Dover, New York, 1961, p. 288.
2 R.D. Gretz, Surf. Sci., 5 (1966) 239.

3 A. Scheludko, Colloids Surfaces, 7 (1983) 81.
4 A. Scheludko, V. Chakarov and B. Toshev, J. Colloid Interface Sci., 82 (1981) 83.
5 A. Scheludko, Colloids Surfaces, 1 (1980) 191.
6 A. Scheludko, B. Toshev and D. Platikanov, in Modern Theory of Capillarity, Akademie Verlag, Berlin, 1981, pp. 163–182; Ann. Univ. Sofia, Fac. Chem., 71 (1976/1977) 111.
7 A. Scheludko, B. Toshev and D. Platikanov, Proc. 31st IUPAC Congress, Sofia, 1987, p. 180.

Pergamon

PII: S0013-4686(96)00151-X

Electrochimica Acta, Vol. 42, No. 2, pp. 251–254, 1997

0013-4686/97 $17.00 + 0.00

Magnetic field effect on copper electrodeposition in the Tafel potential region

V. C. Noninski

Laboratory LEPGER, 149 West 12th Street, New York, NY 10011, U.S.A.

(Received 18 March 1996)

Abstract—Experimental results are reported indicating that a constant homogeneous magnetic field of 12 kGs causes a decrease of the copper deposition overpotential (increase of copper deposition rate) in the Tafel potential region. The experimental results presented in this paper were initially submitted to this journal on 13 December, 1988 as a continuation of the studies in C. Noninski *et al.*, 33rd ISE meeting, **1**, 939 (1982) [1], V. Noninski *et al.*, Elektronnaya obrabotka materialov, **1**, 50 (1986) [2]. Thus, the effect of magnetic field on copper electrodeposition in the Tafel potential region has been established prior to the paper J. P. Chopart *et al.*, electrochim. Acta **36**, 459 (1991) [3], which does not appear to have been recognized in the latter.

Key words: electrode kinetics, magnetic field, copper electrodeposition, electrode overpotential, Tafel potential region

INTRODUCTION

The effect of magnetic field (m.f.) on electrochemical reactions has been the subject of many investigations [1, 2, 4–28]. The main interest in most of these investigations is directed toward the regions where the rate-determining step of the reaction is diffusion (or at least, region of mixed kinetics). The interest in these types of electrode reactions is natural because m.f. is expected to have an effect on the concentration gradients existing in the solution at these conditions.

For the first time the effect of m.f. on the overpotential, η, in the Tafel potential region where the effect of concentration gradients on the overpotential is not expected, was reported in Refs [1, 2].

In the present paper further studies concerning m.f. effects on the copper deposition overpotential in the Tafel region are presented. Copper electrodeposition from sulfuric acid solutions is chosen for this study because of its technological significance and because of the fact that a well expressed Tafel potential region exists in which it is well established that the reasons for the overpotential are pure kinetic (see for instance the classical paper of Mattsson and Bockris [29]).

EXPERIMENTAL

In Fig. 1 the experimental set-up is shown schematically. The disc-shaped electrolytic copper cathode of 0.1 cm^2 working surface area and anode (also of electrolytic copper) of $\sim$20 cm^2 surface area are situated in a quartz cuvette of $2 \times 2 \times 3$ cm^3 dimensions. A saturated calomel electrode (*sce*) is used as a reference electrode. Sulfuric acid solutions of $CuSO_4$ were made using bidistilled water and chemicals of p.a. grade. The electromagnet used is of 12 kGs induction with a 3 cm gap between the poles.

In Fig. 2 another set-up used is shown, enabling the Luggin capillary of $\sim$30 μm diameter to be set at strictly chosen distances from the electrode surface.

The constant current is maintained using Radelkis OH-405 (Hungary) potentiostat–galvanostat used as galvanostat and the overpotential is measured using lamp millivoltmeter СП-2 (Fig. 2). The current–time transients were recorded on Endim 620.01 (GDR) X–Y recorder.

RESULTS

In Fig. 3 an example of overpotential–time transient is shown, taken while keeping constant the current passing through the electrolytic cell. The current corresponds to a potential from the Tafel potential region. From Fig. 3 it is seen that when the m.f. is turned on the copper deposition overpotential rapidly decreases to reach a minimum value. After that a slow increase of the overpotential is observed until a constant value is reached. The stationary overpotential value is much lower than the magnetic-field-off value of the overpotential. At higher currents (also corresponding to the Tafel potential region) the stationary magnetic-field-on value of the overpotential is attained much faster, shortly after the moment

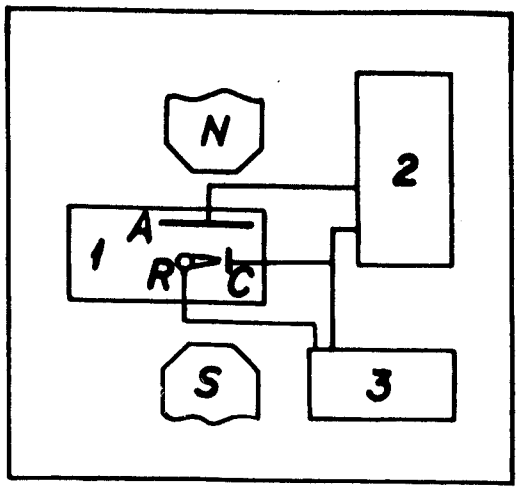

Fig. 1. Scheme of the experimental set-up for measuring the effect of magnetic field on overpotential (rate) of copper electrodeposition. 1, electrolytic cell; 2, potentiostat–galvanostat Radelkis OH-405 (Hungary): 3, X–Y and Y–t recorder Endim 620.01 (GDR). A, anode; C, cathode, and R, reference electrode. N and S, poles of the electromagnet.

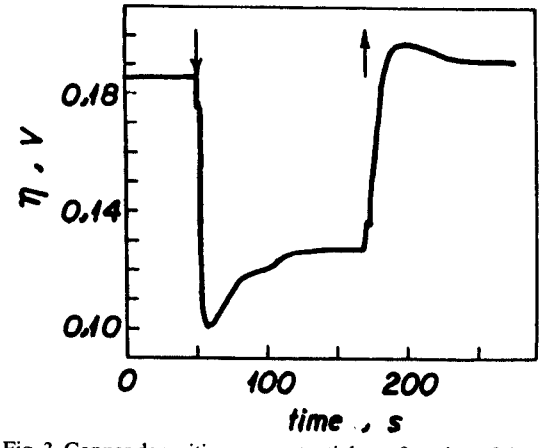

Fig. 3. Copper deposition overpotential as a function of time at current density $i = 0.05$ A cm^{-2} corresponding to the Tafel potential region. ↓, magnetic field on (12 kGs): ↑, magnetic field off. Electrolyte is 0.75 M $CuSO_4$ + 2 M H_2SO_4. The curve is obtained with the experimental set-up shown schematically in Fig. 1.

of turning the m.f. on. After turning off the m.f. the overpotential sharply increases reaching a maximum value, higher than the initial one. After a certain time, the stationary overpotential value after turning off the m.f. becomes equal to the initial overpotential value. At higher current densities (c.d.s) the maximum disappears and after turning the m.f. off the overpotential reaches its steady-state value without exceeding its initial one.

In Fig. 3 some other peculiarities in the run of the curve are seen which to a different extent appear with all the curves taken at the various c.d.s corresponding to the Tafel potential region. We shall not comment on them here.

Curves of the type shown in Fig. 3, taken at different currents, are used to obtain Fig. 4. From every such curve the stationary value of the overpotential in the presence and in the absence of m.f. is plotted against the corresponding current density.

From Fig. 4 it is seen that when the m.f. is off, the dependence between the overpotential, η, and log i is linear, *ie* it obeys the Tafel law:

$$\eta = a + b \log i \qquad (1)$$

where a and b are constants and i is the applied current density.

It is seen from Fig. 4 that the m.f. causes the overpotential to decrease (the reaction rate to increase), this decrease being higher at the higher c.d.s. The overpotential decrease observed in Fig. 4 is of the order of the decrease when applying continuous mechanical renewal (CMR) of the

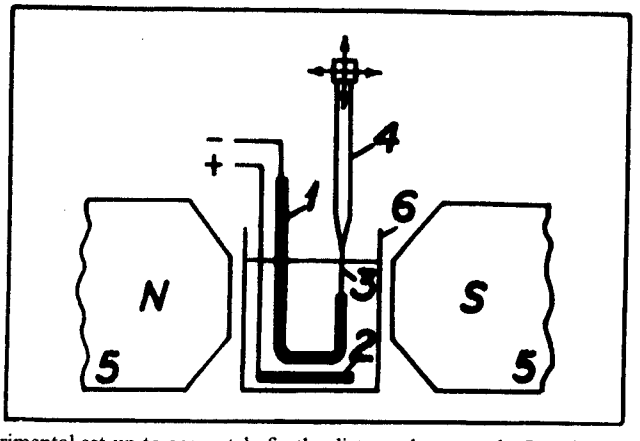

Fig. 2. Scheme of the experimental set-up to accurately fix the distance between the Luggin capillary tip and the electrode surface. 1, copper cathode ($S = 0.1$ cm^2): 2, copper anode ($S \approx 10$ cm^2); 3, Luggin capillary ($d \approx 30$ μm); 4, saturated calomel electrode attached to a micrometric table (not shown in the figure); 5, electromagnet of 12 kGs induction; 6, quartz cuvette.

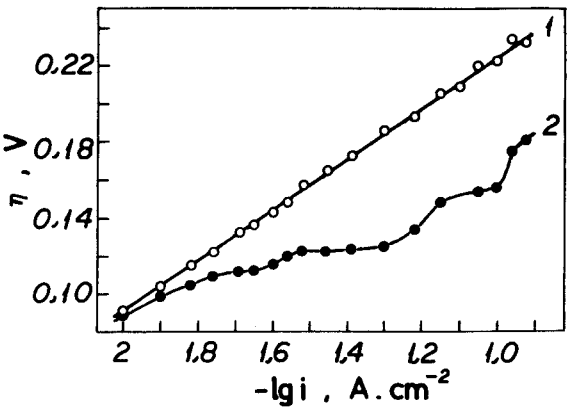

Fig. 4. Tafel plot for the electrodeposition of copper from 0.75 M $CuSO_4$ + 2 M H_2SO_4 obtained with the experimental set-up shown schematically in Fig. 1, line 1. Curve 2, η–log i dependence in the presence of a magnetic field of 12 kGs. This figure is obtained on the basis of transients similar to those shown in Fig. 3, taken at various current densities.

electrode surface—about 0.060 V at the higher c.d.s [30]. The slope of the Tafel line, b, in the absence of m.f. is ~0.130 V which is in agreement with the observed value of b in [17]. When the m.f. is on, the run of the η–log i line changes. One can hardly consider that the linear dependence is preserved any more; the line is transformed into a curve situated at lower overpotentials. Therefore, according to Fig. 4, in m.f. the Tafel dependence is no longer observed; it looks as if the Tafel dependence is being "destroyed". It is interesting to note that a similar "destroying" of the linearity between η and log i is observed (though unnoticed by the authors) in Fig. 5 of [28]. One can see in Fig. 5 of [28] that the linear η–log i dependence under m.f. is shortened and the points corresponding to the higher c.d. values do not lie on the Tafel line.

From Fig. 5 it is seen that when removing the Luggin capillary away from the electrode surface the change of the potential (overpotential) is significantly greater than that corresponding to the Ohmic drop. For distances greater than about 0.2 cm evidently it is the Ohmic component of the potential, due to the resistance of the solution, that determines the run of the η–d curve. This fact is in agreement with the earlier observed dependence between the electrode potential and d [31]. With the increase of the c.d. the change of the overpotential with the distance d is more clear. In m.f. of 12 kGs a change in the run of the η–d curve is observed which is greater the greater is the polarizing current.

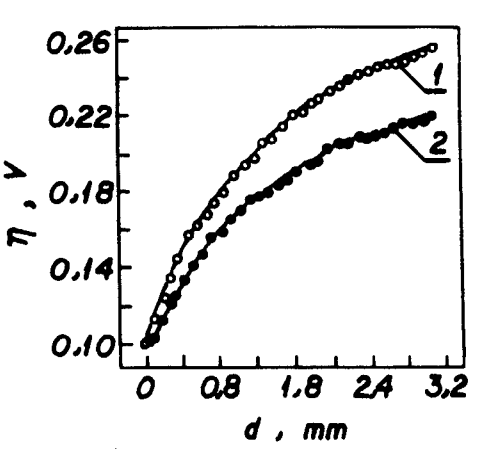

Fig. 5. Copper deposition overpotential as a function of the distance, d, between the Luggin capillary tip and the electrode surface. The curves are obtained with the set-up shown schematically in Fig. 2. Solution, 0.75 M $CuSO_4$ + 0.1 M H_2SO_4; 1, magnetic field is off; 2, magnetic field of 12 kGs is on. Current density i = 0.05 A cm^{-2}.

It is seen from Fig. 5 that at every distance, d, between the electrode and the capillary, at the given c.d. value, the overpotential value obtained in the presence of m.f. is always lower than in absence of m.f. This observation is in agreement with the conclusions from Fig. 4.

The dependencies shown in Fig. 4 correspond to a certain distance, d, between the capillary and the electrode surface. We can determine that distance at which the Luggin capillary is during the experiment. Thus, from Fig. 4, the overpotential value is determined, corresponding to the c.d. at which, say, curve 1 in Fig. 5 is obtained, and then from Fig. 5 the distance, d, to which this overpotential corresponds is worked out.

Unfortunately, because of the difference of the H_2SO_4 concentrations at which Figs 4, 5 were obtained the determination of d in the present case will not be exact. Here, we only mention the principle as a possibility for such determinations.

As is seen from Fig. 5 the effect of m.f. is felt in the bulk of the solution, beyond the double electric layer, rather than at the very electrode–electrolyte interface. This can be considered as an indication that the cause of the overpotential should be looked for on the side of the solution, at a macroscopic level. The change of the overpotential observed in Fig. 5 is connected with the decrease of the Ohmic drop in the solution layer between the capillary tip and the surface of the

cathode. The sole cause for the observed decrease of the Ohmic resistance must be the change of the solution concentration in the solution layer near the electrode (*ie* decrease of the copper ion concentration in the layer near the electrode, in the direction towards equalizing it with its concentration in the bulk of the solution at unchangeable concentration of the sulfuric acid). Evidently, under the action of the magnetic field the ions change their trajectory of movement due to the Lorentz force in such a way that their concentration in the solution layer near the electrode decreases. Discussion in more detail of how this concentration change may affect the activation overpotential will be given elsewhere.

Our experiments [1] unlike the observations in [28] showed that the m.f. influence on Cu deposition overpotential depends on the cathode surface orientation with respect to the magnetic field lines of force. When the cathode surface is perpendicular, and accordingly the lines of current are parallel to the magnetic lines of force, no influence of the m.f. on the overpotential is observed. Further, the m.f. influence on the overpotential does not depend on the mutual cathode–anode orientations (and respectively on the corresponding disposition of the current lines). It seems the influence of the m.f. is concentrated on the ions situated at a very close distance from the cathode surface, where the direction of the ion motion does not depend on the mutual cathode–anode surface orientations.

As noted, in the present paper no attempts to explain the observed effects will be made, these will be deferred to future communications. It will only be noted that the claim in [21] that the m.f. may affect the rate of both activation (charge-transfer) and mass-transport controlled processes has not been proven. In [21] a case is observed in which m.f. induces potential difference (causes current to flow) in a flowing electrolyte system. It is also to be noted that the authors of [28], who also observe m.f. effects on the activation overpotential of copper deposition (and who also fail to recognize in their paper the prior establishment of this effect in [1, 2]) look for the reasons for this effect in terms of mass-transport effects, although the nature of the overpotential is discussed by them according to the charge-transfer theory.

REFERENCES

1. C. Noninski, V. Noninski and V. Terzyiski, 33rd ISE meeting, Lyon, France, Vol. 1. p. 939 (1982).
2. V. Noninski and C. Noninski, *Elektronnaya obrabotka materialov* (USSR) **1,** 50 (1986).
3. J. P. Chopart, J. Douglade, P. Fricoteaux and A. Oliver, *Electrochim. Acta* **36,** 459 (1991).
4. E. J. Center, R. C. Overbeck and D. L. Chase, *Anal. Chem.* **23,** 1134 (1951).
5. L.. Yang, *J. Electrochem. Soc.* **101,** 456 (1954).
6. A. M. Evseev, *Zhurnal Fizicheskoi Khimii* (USSR) **36,** 1610 (1962).
7. E. Z. Gak, *Elektrokhimia (USSR)* **3,** 263 (1967).
8. D. Guerin-Ouler, C. Nicollin and A. Olivier, *C.R. Acad. Sci. Paris* **270,** 1500 (1970).
9. S. Mohanta and T. Z. Fahidy, *Can. J. Chem. Engin.* **50,** 248 (1972).
10. D. Laforgue-Kantzer, A. Laforgue and T. Cong Khanh, *Electrochim. Acta* **17,** 151 (1972).
11. J. Dash and W. W. King, *J. Electrochem. Soc.* **119,** 51 (1972).
12. M. Ammar, A. Laforgue and D. Laforgue-Kantzer, *C.R. Acad. Sci. Paris* **274,** 2140 (1972).
13. T. Z. Fahidy, *Electrochim. Acta* **18,** 607 (1973).
14. E. Z. Gak, E. H. Rokhinson and N. F. Bondarenko, *Elektronnaya obrabotka materialov* (USSR) **6,** 24 (1973).
15. S. Mohanta and T. Z. Fahidy, *Electrochim. Acta* **19,** 771 (1974).
16. S. Mohanta and T. Z. Fahidy, *Electrochim. Acta* **19,** 835 (1974).
17. E. Z. Gak, E. Kh. Rokhinson and N. F. Bondarenko, *Sov. Electrochem.* **11,** 489 (1975).
18. E. Z. Gak, E. Kh. Rokhinson and N. F. Bondarenko, *Sov. Electrochem.* **11,** 495 (1975).
19. A. P. Shorigin, G. L. Danielyan and R. Z. Alimova, *Elektrokhimia* (USSR) **11,** 1478 (1975).
20. V. N. Duradji and I. V. Bryantzev, *Elektronnaya obrabotka materialov* (USSR), **15,** 235 (1976).
21. E. J. Kelly, *J. Electrochem. Soc.* **124,** 987 (1977).
22. M. I. Ismail and T. Z. Fahidy, *Can. J. Chem. Engin.* **58,** 505 (1980).
23. G. Neite and E. Nembach, *Mater. Sci. Eng.* **52,** 169 (1982).
24. R. N. O'Brien and K. S. V. Santhanam, *J. Electrochem. Soc.* **129,** 1266 (1982).
25. A. Chiba, H. Hosokawa and T. Ogawa, *Surf. Coat. Technol.* **27,** 131 (1986).
26. A. Chiba, T. Niimi, H. Kitayama and T. Ogawa, *Surf. Coat. Technol.* **29,** 347 (1986).
27. A Chiba, K. Kitayama and T. Ogawa, *Surf. Coat. Technol.* **27,** 83 (1986).
28. A. Chiba, T. Ogawa and T. Yamashita, *Surf. Coat. Technol.* **34,** 38 (1988).
29. E. Mattsson and J. O'M. Bockris, *Trans. Faraday Soc.* **55,** 1586 (1959).
30. C. Noninski, L. Veleva and V. Noninski, *Surf. Technol.* **25,** 127 (1985).
31. C. Noninski, 33rd ISE meeting, Lyon, France, Vol. 1, p. 933 (1982).

Corrosion Science, Vol. 30, No. 8/9, pp. 839–847, 1990
Printed in Great Britain

0010-938X/90 $3.00 + 0.00

CORROSION STUDIES WITH THE SELF-CLEANING ROTATING ELECTRODE (SRE)

V. C. NONINSKI

Higher Institute of Chemical Technology, Laboratory on Electrochemistry of Renewed Interface (LEPGER), Sofia 1156, Bulgaria

Abstract—Current–time curves taken with the self-cleaning rotating electrode (SRE) are applied to study the transition from the state of continuously mechanically renewed (CMR) electrode surface to that of non-renewed surface of some steels, noble metals, Pt and Cu. These curves make it possible to characterize quantitatively both the common features and the peculiarities of that transition for different metals in corrosive media. It is also possible, on the basis of these current–time transients, to characterize quantitatively the action of inhibitors of metal corrosion in a dynamic regime, unlike the commonly used steady-state degree of protection from corrosion. The experimental findings on the basis of these curves can further be used for establishing the mechanism and kinetics of active dissolution, passive layer formation, the inhibiting of metal corrosion by different substances etc. These transients can accompany the produced metals and inhibitors and also can be gathered together in an Atlas, to help engineers choose the most suitable metal or inhibitor when their construction is to undergo mechanical stress, strain, vibrations etc., i.e. when a fresh metal surface is expected to appear.

INTRODUCTION

THE METHOD of continuous mechanical renewal (CMR) of the electrode surface with the help of the self- cleaning rotating electrode (SRE)[1] is suitable for examining the corrosion behaviour of metals in cases where there is contact of fresh metal surface with a corrosive medium. There are studies in literature of the effect of mechanical factors (scratching, wiping etc.) on the corrosion behaviour of metals[2–50] which help towards an understanding of the mechanism of passivation, stress corrosion etc. Before SRE, however, it was not possible for the effect of CMR to be studied under: (a) defined conditions of the surface—constant surface area, controllable state of renewal, renewing of the whole surface which is unscreened by the renewing device etc.; and (b) diffusion and hydrodynamic conditions of the system which both ensure high reproducibility of the results and enable effects to be observed which are difficult to observe in any other way, for example, the effect of the hydrogen evolution overvoltage decrease during the CMR of metals possessing a high hydrogen overpotential.[51] Results on studies concerning the anodic behaviour of some steels, a noble metal, Pt, Cu and of some inhibitors of corrosion in the conditions of continuous mechanical renewal (CMR) of the anode surface are presented below.

EXPERIMENTAL METHOD

Two main types of experiment have been carried out. One consisted of determining the polarization curves on non-renewed surface and comparing them with the polarization curves taken in the same conditions but during the CMR of the surface. Another was the registration of time and potential transients by applying a potential to the anode while the latter is under CMR conditions; the change of

Manuscript received 25 April 1988; in amended form 1 July 1988 and 18 April 1989.

current with time is registered. At a certain moment the renewal of the surface is suddenly stopped but the registration of the curve continues. Thus the changes in the current–time curve while the surface passes from the state of CMR to the state of non-renewed surface can be observed. To see what influence a new renewal of the surface will have for some experiments the electrode at a given moment was rotated anew.

Current–time transients upon scratching the surface of the electrode have been reported previously,[12–16,17–19,36–50] as well as earlier studies of transients connected with metal corrosion.[31–33] The potentials at which the transients were registered were obtained from the polarization curves taken at the beginning of the experiment.

EXPERIMENTAL RESULTS AND DISCUSSION

The region of active dissolution

In this region a relatively weak influence of the CMR is observed on the current–time curves of the steels Г13 and Х18АГ12, curves 1 and 2 of Fig. 1. The renewal does not remove the factors which cause an eventual retardation of the dissolution process. From curves 1 and 2 of Fig. 1 it can be seen that the behaviour of the two steels is somewhat different. At curve 1 a fast return to the state of non-renewed surface takes place. At curve 2 the transition to non-renewed surface is smooth and the steady-state is reached after a significant interval of time. The specimens of the steels manufactured by the Japanese firms show a significant influence of the CMR in this range of potentials. Though the specimens are of the same trade mark there are certain differences in the technology of their production. It should be noted that the current–time curves are taken at differing potentials though these potentials are all chosen to be near the maximum of dissolution of the different steels. This fact probably also has its influence on the curves.

For curve 1 in Fig. 2, obtained in H_2SO_4, stopping the renewal causes a fast drop of the current which becomes cathodic. However, immediately afterwards the cathodic current begins to decrease again eventually becoming anodic with a

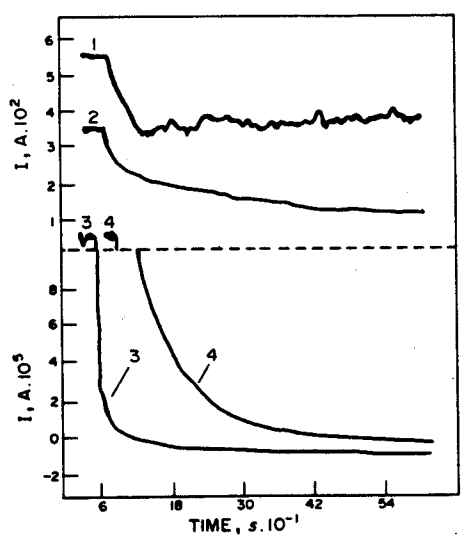

FIG. 1. Current–time transients for various steels at potentials near the maximum of the anodic dissolution in the active region: (1) Г13 (composition: C—0.95, Mn—11.88, Si—1.28, N_2—0.0254%), ϕ = −0.120 V(NHE); (2) Х18АГ12 (C—0.053, Mn—11.14, Cr—17.94, Si—0.8, N_2—0.448%), ϕ = −0.220 V(NHE); (3) AISI 304, NISSHIN Steel Co., ϕ = +0.230 V(NHE); (4) AISI 304 NIPPON JAKIN, ϕ = +0.280 V(NHE).

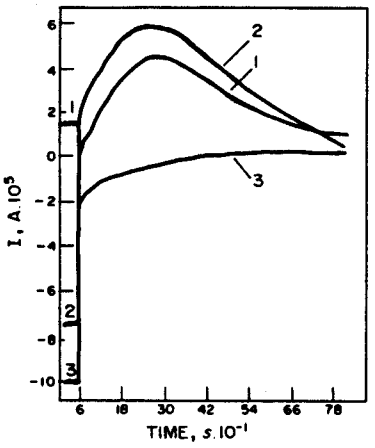

FIG. 2. Current–time dependencies obtained at potential $\phi = -0.11$ V. Anode—stainless steel 1X18H9T. (1) 8 N H_2SO_4; (2) 8 N H_2SO_4 + $K_2Cr_2O_7$; (3) 8 N H_2SO_4 + $KMnO_4$. The concentration of the inhibitors in all cases was 1%.

maximum. After the addition of $K_2Cr_2O_7$, a cathodic current passes through the electrode during CMR. After stopping the renewal the cathodic current rapidly decreases and also becomes anodic, also passing through a maximum. Curve 3 obtained after the addition of $KMnO_4$ upon CMR is situated at even higher cathodic current than curve 2 upon CMR. When the renewal is stopped curve 3 does not pass into the anodic region. Passing of the current from anodic into cathodic after ceasing of the renewal shows that the anodic dissolution entirely stops. The rapid transformation of the cathode current again into an anode one can be explained by the effect of the cathode process on the state of the electrode surface and eventually also on the inhibitor present on the electrode surface which again causes activation of the electrode. The maxima of curves 1 and 2 are connected with the fact that the changes in the state of the electrode surface at the anode process are opposite to the changes when a cathodic process takes place.

From curve 1 of Fig. 3 the Pt electrode exhibits a current of $\sim 4 \times 10^{-6}$ A which flows through the SRE. Investigation showed[52] that this anodic current at a similar potential is due to anodic dissolution of Pt. After stopping the renewal the current decreases to reach a steady-state value practically equal to zero. On re-starting the renewal the current rapidly increases reaching the starting value. Curve 2 in Fig. 3 shows that the addition of $K_2Cr_2O_7$ leads to an increase of the anode current value of almost an order of magnitude on renewal. After stopping the renewal in this case the anode current rapidly decreases to a minimum value after which it begins to increase to reaching a steady-state value greater than the one in pure H_2SO_4. Curve 3 in Fig. 3 shows that the addition of $KMnO_4$ during CMR exerts a diametrically opposite influence on the anode process in comparison with $K_2Cr_2O_7$—the anodic current decreases down to zero and even passes to the cathode, the latter having a value of about two orders of magnitude greater than the anodic current value in pure H_2SO_4. After stopping the renewal the cathode current decreases but does not pass again into anodic one. The activation of the Pt surface after the addition of $K_2Cr_2O_7$ and its passivation when adding $KMnO_4$ can be explained if it is accepted that in H_2SO_4

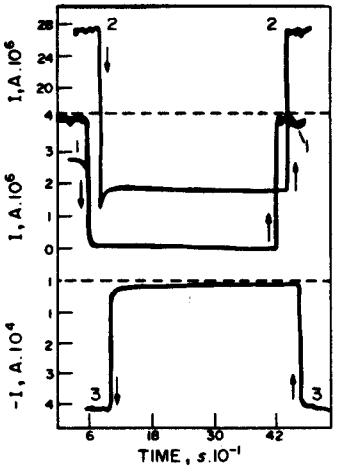

FIG. 3. The dependence of the current passing through Pt SRE on the time at potential 1.08 V(NHE). (1) N H_2SO_4; (2) 1 N H_2SO_4 + $K_2Cr_2O_7$; (3) 1 N H_2SO_4 + $KMnO_4$. Rate of SRE rotation 1000 rpm. ↓—rotation of the SRE (renewal) is ceased. ↑—rotation of the SRE (renewal) begins (1000 rpm).

solution at a potential of 1.080 V, though lower than the equilibrium potential of the oxygen electrode, the same passivating layer begins to appear on the Pt surface which preserves the latter from dissolution at potentials higher than the equilibrium potential of the oxygen electrode; the $K_2Cr_2O_7$ hinders while $KMnO_4$ helps the formation of a passivating layer. It should be expected that the presence of $K_2Cr_2O_7$ and $KMnO_4$ exerts certain influence on the composition of the passivating layer.

This suggestion is consistent with the current–time curves obtained in 1 N KOH and shown in Figs 4–6. From Fig. 4 it is seen that $K_2Cr_2O_7$ and $KMnO_4$ act directly on

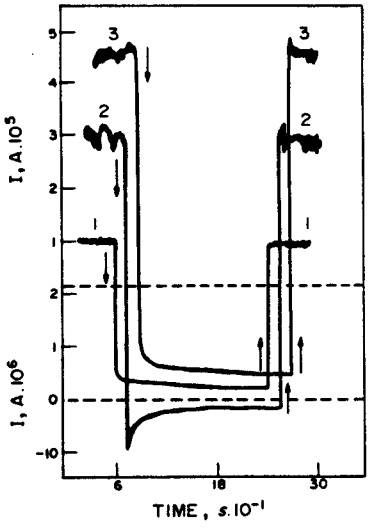

FIG. 4. Current–time dependencies on Pt SRE polarization at potential 0.14 V(NHE). (1) 1 M KOH; (2) 1 M KOH + $K_2Cr_2O_7$; (3) 1 M KOH + $KMnO_4$.

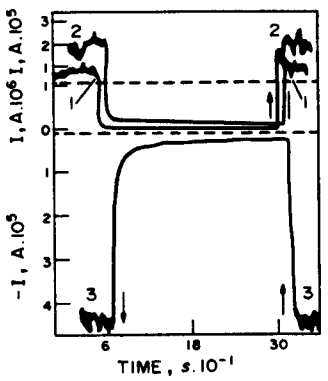

FIG. 5. Current–time dependencies on Pt SRE polarization at potential of 0.240 V(NHE). (1) 1 M KOH; (2) 1 M KOH + $KMnO_4$; (3) 1 M KOH + $K_2Cr_2O_7$.

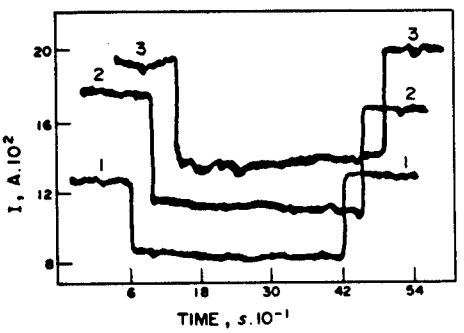

FIG. 6. Current–time dependencies on Pt SRE polarization at 1.240 V potential. (1) 1 M KOH; (2) 1 M KOH + $KMnO_4$; (3) 1 M KOH + $K_2Cr_2O_7$.

the passivating layer upon CMR as common oxidizers and accelerate the dissolution. At a potential nearer to the equilibrium oxygen the curves in Fig. 5 show that the passivating layer already begins to form and an influence on that formation adds to the direct influence on the rate of Pt dissolution. This influence is the same as in Fig. 3 though here the roles of $KMnO_4$ and $K_2Cr_2O_7$ are exchanged. At 1.24 V the formation of the passivating layer does not seem to be influenced by the presence of $K_2Cr_2O_7$ and $KMnO_4$ and they manifest themselves as common oxidizers, again accelerating, though weakly, the Pt dissolution.

From curves 1 and 4 in Fig. 7, taken at potentials from the region of active dissolution of Cu, it is seen that after stopping the renewal the transition from the state of CMR surface to the state of non-renewed is relatively slow. At a potential corresponding to the maximum of the dissolution rate—curve 2—this transition is already rapid.

The passive region

From curve 3 in Fig. 7 the transition from the state of CMR to the steady-state of non-renewed surface can be seen to take place more rapidly than the corresponding

transition in the region of active dissolution. Clearly, if passivation is promoted, by, for example, sedimentation of $CuSO_4$, as a result of the supersaturation at the anode layer, the current will decrease much more rapidly than in the absence of such a factor.

From curve 1 in Fig. 8 it is seen that the depth of passivation of X18АГ12 is the greatest for the studied steels in this figure. Despite this fact, however, for some uses

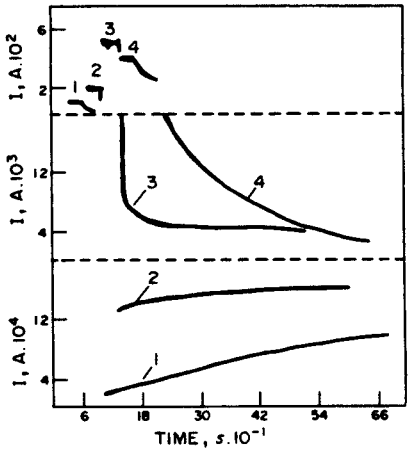

FIG. 7. Current–time transients of Cu SRE in 0.49 M $CuSO_4$ + 4 M H_2SO_4. Curve (1) is taken at 0.44 V; (2) 0.58 V; (3) 0.68 V; (4) 0.38 V.

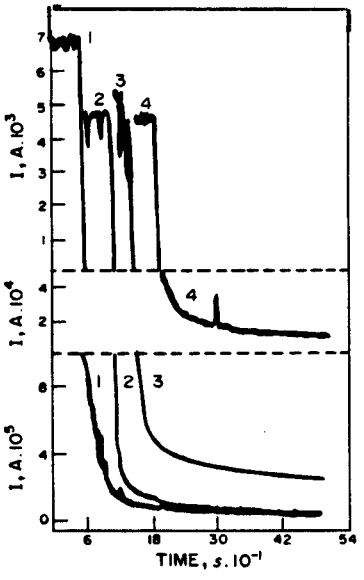

FIG. 8. Current–time dependencies for various steels, obtained with the help of the SRE in 8 N H_2SO_4 at potentials from the passive region of these steels (where the passivation is deepest). (1) X18АГ12, ϕ = +0.680 V(NHE); (2) AISI 304 NISSHIN Steel Co., ϕ = 0.780 V; (3) AISI 304 NIPPON JAKIN, ϕ = +0.730 V, (4) Г13, ϕ = +0.178 V. Compositions of the steels are the same as in Fig. 1.

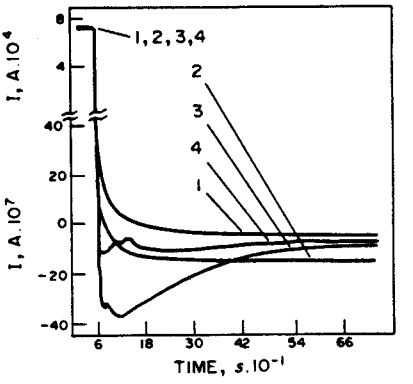

FIG. 9. Current–time dependencies obtained at potential ϕ = +0.480 V. Anode—stainless steel 1X18H9T. (1) 8 N H_2SO_4; (2) 8 N H_2SO_4 + $K_2Cr_2O_7$; (3) 8 N H_2SO_4 + $KMnO_4$; (4) 8 N H_2SO_4 + $KMnO_4$ + H_3PO_4.

the steel corresponding to curve 2 might be preferred because passivity is reached more rapidly. Peaks can be seen in curve 1 which are an indication for a certain tendency towards depassivation. Γ13 steel also exhibits a tendency towards depassivation. According to the current–time curves the steels produced in Japan do not differ much from one another but the depth of passivation of the steel produced by NISSHIN Steel Co. is greater. The curves also do not differ much in the region of CMR. In the active region a full corrosion protection of the Japanese steels takes place: the curves in Fig. 1 change from anodic to cathodic. In the passive region such an effect is not observed with these steels.

In Fig. 9, unlike Fig. 2, the current on CMR is the same in the absence and presence of inhibitors. After stopping the renewal the current rapidly decreases becoming cathodic , this change being fastest with $KMnO_4$ which also causes the cathode current to pass through a maximum. Curve 4 in Fig. 9 shows that when H_3PO_4 is added the influence of the $KMnO_4$ significantly decreases. The experiments showed that some other inhibitors such as pyridine, HNO_3, piperidine, β-naphthol, phenol, benzene, benzaldehyde, aniline, α-naphthylamine, picric acid, anthraquinone, benzoic acid, etc. do not influence the run of curve 1 of Fig. 9. The fact that at a potential in the passive region on renewal of the surface the inhibitors do not influence the current value shows that the observed current is defined practically only by the two processes: formation of the passivating layer and mechanical removal of the layer by CMR. The action of the inhibitors is negligibly small compared to that of the factors determining the formation of the passivating layer. This is seen better from the current–time curves after stopping the renewal of the surface. According to curve 1 of Fig. 9, after stopping the renewal the formation of a passivating layer decreases the current by several orders of magnitude, while according to curves 2–4 compared to curve 1 the additional change of the current under the action of the inhibitors is of the order of a thousandth part from the change due to formation of a passivating layer.

CONCLUSIONS

(1) The transients can be used to estimate the transition from the state of CMR to the state of non-renewed metal electrode surface. Furthermore, the current–time

transients can be used to examine the mechanism and kinetics of active metal dissolution, the formation of passivating layers, the inhibition of metal corrosion etc.

(2) The characteristics of transients can be an indication for the corrosion properties of metals where a fresh metal surface is created.

(3) Transients can be used for a quantitative characterization of inhibitors of metal corrosion in a dynamic regime, unlike the commonly used steady-state degree of protection from corrosion.

REFERENCES

1. C. I. NONINSKI, *Khimia i industria* (Bulgaria) **38**, 442 (1966).
2. H. ABD EL KADER and S. M. EL TANGY, *Electrochim. Acta* **30**, 841 (1985).
3. A. A. ADAMS and R. T. FOLEY, *Corrosion* **31**, 84 (1975).
4. J. R. AMBROSE and J. KRUGER, *Corrosion* **28**, 30 (1972).
5. E. V. BARELKO and B. N. KABANOV, *Dokl. Akad,. Nauk SSSR* (USSR) **90**, 1059 (1953).
6. T. R. BECK, *J. electrochem. Soc.* **115**, 890 (1968).
7. T. R. BECK, *Electrochim. Acta* **18**, 807 (1973).
8. T. R. BECK, *Electrochim. Acta* **18**, 815 (1973).
9. T. R. BECK, *Electrochemical Techniques for Corrosion* (ed. R. Baboian), p. 27, NACE, (1977).
10. T. R. BECK, *J. electrochem. Soc.* **129**, 2500 (1982).
11. M. W. BREITER, *Electrochim. Acta* **12**, 679 (1967).
12. G. T. BURSTEIN and D. H. DAVIES, *Corros. Sci.* **20**, 1143 (1980).
13. G. T. BURSTEIN and D. H. DAVIES, *J. electrochem. Soc.* **128**, 33 (1981).
14. G. T. BURSTEIN and D. H. NEWMAN, *Corros. Sci.* **20**, 375 (1980).
15. G. T. BURSTEIN and D. H. NEWMAN, *Electrochim. Acta* **25**, 1009 (1980).
16. G. T. BURSTEIN and D. H. NEWMAN, *Electrochim. Acta* **26**, 1143 (1981).
17. F. P. FORD, PhD Thesis, Univ. of Cambridge (1973).
18. F. P. FORD, *Metal Sci.* **12**, 326 (1978).
19. F. P. FORD, G. T. BURSTEIN and T. P. HOAR, *J. electrochim. Soc.* **127**, 1325 (1980).
20. N. M. GONTMAHER, V. E. GUTERMAN, V. A. SAFONOV, O. A. PETRII and V. P. GRIGORJEV, *Elektrokhimia* (USSR), **23**, 3 (1987).
21. K. GOSNER, *Z. phys. Chem.* (NF), **36**, 392 (1963).
22. K. GOSNER, *Z. phys. Chem.* (NF), **42**, 374 (1964).
23. K. GOSNER, U. FREYER and F. MANSFELD, *Z. phys. Chem.* (NF), **42**, 378 (1964).
24. T. HAGYARD and K. M. CHAPMAN, *J. electrochem. Soc.* **113**, 961 (1967).
25. T. HAGYARD and W. B. EARL, *J. electrochem. Soc.* **114**, 694 (1967).
26. T. HAGYARD and M. J. PRIOR, *Trans. Faraday Soc.* **57**, 2295 (1961).
27. T. HAGYARD and J. P. WILLIAMS, *Trans. Faraday Soc.* **57**, 2288 (1961).
28. E. KUNZE and K. SCHWABE, *Corros. Sci.* **4**, 109 (1964).
29. R. A. MACHEVSKAJA and A. V. TURKOVSKAJA, *Khimicheskoe i neftjanoe mashinostroenie* (USSR), No. 4, **32** (1965).
30. R. A. MACHEVSKAJA and A. V. TURKOVSKAJA, *Zhurnal Prikladnoi Khim.* (USSR), **38**, 335 (1965).
31. C. I. NONINSKI, R. G. RAICHEV and Z. L. GEORGIEV, *Khimia i industria* (Bulgaria), **45**, 220 (1973).
32. C. I. NONINSKI, R. G. RAICHEV and Z. L. GEORGIEV, *Khimia i industria* (Bulgaria), **45**, 311 (1973).
33. C. I. NONINSKI, R. G. RAICHEV and Z. L. GEORGIEV, *Khimia i industria* (Bulgaria), **45**, 407 (1973).
34. C. I. NONINSKI and V. C. NONINSKI, *8th International Congress on Metallic Corrosion* v. 2, p. 1251. Mainz, FRG (1981).
35. C. I. NONINSKI and V. C. NONINSKI, *Mashinostroene* (Bulgaria), No. 7, 316 (1982).
36. R. C. NEWMAN and G. T. BURSTEIN, *Corros. Sci.* **21**, 119 (1981).
37. F. OEHME and H. RHYN, *Mesures*, **34**, 81 (1969).
38. H. DIETZ and H. GOEHR, *Z. phys. Chem.* **223**, 113 (1963).
39. W. POPP, *Electrochim. Acta* **8**, 361 (1963).
40. M. PRAZAK, E. BERANEK and K. KARNIK, *J. Phys. Chem.* **214**, 299 (1962).
41. G. RADLEIN, *Z. Elektrochem.* **61**, 727 (1957).
42. K. SCHWABE, *Electrochim. Acta* **3**, 186 (1960).
43. K. SCHWABE, *Z. phys. Chem.* **214**, 343 (1960).

44. K. SCHWABE, and G. DIETZ *Z. Electrochem.* **62**, 751 (1958).
45. K. SCHWABE, *Werkstoffe Corros.* **1**, 70 (1964).
46. N. D. TOMASHOV, G. P CHERNOVA, R. M. AL'TOVSKII and G. K. BLINCHEVSKII, *Zavod. Lab.* (USSR), **24**, 299 (1958).
47. N. D. TOMASHOV, N. M. STRUKOV and L. P. VERSHININA, *Electrokhimia.* (USSR), **5**, 26 (1969).
48. N. D. TOMASHOV and L. P. VERSHININA, *Electrochim. Acta* **15**, 501 (1970).
49. N. D. TOMASHOV and L. P. VERSHININA, *Novie Metodi Issledovanija Korozii Metalov*, p. 64. Nauka, Acad. Nauk SSSR Moscow, USSR (1973).
50. R. C. NEWMAN, *Corrosion Chemistry Within Pits, Crevices and Cracks* (ed. A. Turnbull). HMSO, London (1987).
51. C. I. NONINSKI, I. P. IVANOV and M. VASSILEVA-DIMOVA, *J. electrochem. Soc.* **130**, 1836 (1983).
52. V. C. NONINSKI, Dissertation, Higher Inst. Chem. Tech. Sofia (1983).

J. Electroanal. Chem., 267 (1989) 287–290
Elsevier Sequoia S.A., Lausanne – Printed in The Netherlands

Short communication

Underpotential anodic dissolution of noble metals during the continuous mechanical renewal of their surface

V.C. Noninski

Laboratory for Electrochemistry of Renewed Electrode–Solution Interfaces (LEPGER), P.O. Box 9, Sofia 1504 (Bulgaria)

(Received 16 March 1989)

INTRODUCTION

During the anodic polarisation of Pt it is possible for anodic dissolution to take place [1–12]. Furthermore, it has been established by us [13] that, during the continuous mechanical renewal (CMR) of the anode surface, the noble metals (Pt, Rh, Au) and their alloys are dissolved anodically at rates commensurate with the rates of the anodic dissolution of the base metals whose surface is not renewed. Potential regions exist, however, where because of thermodynamic reasons, electrochemical dissolution of non-renewed Pt is impossible. During studies of the anodic evolution of oxygen during the CMR of Pt anodes it has been established [14] that at potentials lower than that at which it is thermodynamically possible for electrochemical dissolution of platinum to take place, significant anodic currents are observed. Some preliminary experiments have shown that besides the passing of a capacitance current, in this case anodic dissolution of the noble metal takes place [15]. The aim of the present communication is to present some experimental evidence for such dissolution.

EXPERIMENTAL

The experiments were carried out using the self-cleaning rotating electrode (SRE) [16]. The cone-shaped working surface of this electrode is presented against four sharp edges of a device called a sharpener, made of baked corundum. When the electrode is rotated, its conical surface is continuously renewed mechanically by these edges. The pressure of the electrode surface against the sharpener's edges can be controlled during the experiment through a scale connected to a spring or by using heavy washers of known weight. The extent of renewal is controlled by the rate of rotation of the SRE. During the renewal the surface of the electrode is practically unscreened. When the electrode is not rotated, the conical surface works

0022-0728/89/$03.50

as a common conical stationary electrode. The experiments were carried out mainly with a spectrally pure platinum (Johnson Matthey) electrode. The experimental setup was similar to that described in ref. 14, the anode compartment being isolated from the cathode one by a salt bridge to prevent the Pt ions eventually appearing from passing into the cathode compartment and being reduced there. The sulphuric acid solutions in the anodic compartment of the cell before and after the polarisation of the anode were studied by spectroscopy for the presence of Pt ions by the method of Piercy and Ryan [17,18] with a Perkin-Elmer 137 spectrophotometer. As a reagent, *p*-dimethylaminobenzylidenerhodanine (DMABR) with phenylmethyl-*p*-hexadecylammonium chloride (CETYL) added, was used. Firstly, an absorbance vs. Pt^{2+} concentration standard line was constructed by analysing a series of solutions of known Pt^{2+} concentration prepared according to refs. 17 and 18.

RESULTS AND DISCUSSION

There are different methods for determining the amount of platinum in solutions. In the present case, however, in the solution there will be Pt in the atomic state due to the mechanical scraping and eventually Pt in the ionic state due to anodic dissolution. Therefore, in order to prove anodic dissolution it is necessary to determine only the amount of Pt ions in the solution, while leaving the scraped Pt, also present in the solution, undetermined.

A reliable method for the above aim is spectroscopy in the visible region. The experiments began by applying the procedures outlined in refs. 17 and 18 to a blank H_2SO_4 probe. This probe did not show any coloration, which is a guarantee that no Pt ions exist in the solution. This initial H_2SO_4 was transferred to the cell, the electrode rotated and a potential applied. We carried out experiments at two potentials, 0.78 and 0.80 V (SHE) (at pH = 0), in the "immune" region in the Pourbaix diagram of Pt [19]. At certain moments, samples of the solution were taken and studied for the presence of Pt^{2+} according to the procedure described in refs. 17 and 18. The samples showed a pink to red coloration depending on the time of polarisation. The solutions studied demonstrated the characteristic absorption spectrum of the Pt(II)–DMABR complex with a maximum at $\lambda = 520$ nm, corresponding to different absorbance values depending on the amount of Pt^{2+} complex. The coloration was distinct and its appearance could be attributed solely to the existence of Pt ions in the solution, any other reason being excluded. For instance, the particles scraped from the electrode cannot be a source of Pt^{2+} since they are not under the applied anodic potential and the Pourbaix diagram shows the impossibility of Pt dissolution in such a state. Experiments were also carried out in which the electrode was renewed for hours in the solution without potential application. In these experiments no Pt ions were found in the solution.

In Fig. 1 the determined concentration of Pt^{2+} as a function of the time of polarisation of the CMR Pt anode is shown. Due to the mechanical wear of the sharpener's edges caused by the long duration of the experiment, the conditions of

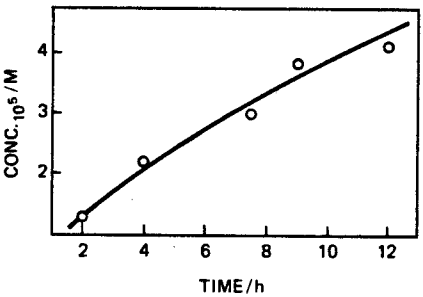

Fig. 1. Concentration of Pt^{2+} as a function of polarisation time in hours. Potential of the electrode 0.78 V vs. SHE.

renewal change, which is one of the reasons for the non-linearity of the dependence in Fig. 1.

Our experiments show [13] that the anodic current increases up to a certain limit with increasing pressure of the electrode surface against the sharpener's edges, after which there is no pressure effect on the current. The effect of the rotation speed on the observed anode current [13] is similar: with an increase of the electrode rotation rate the current increases until a certain limiting value is reached which remains constant when the rotation speed is increased further. In the present investigations the pressure of the sharpener's edges was maintained at 0.8–0.9 N cm^{-1} of edge length and was kept constant during the whole course of the experiment, while the electrode rotation speed was 1000 rpm; these values of pressure and rotation speed were chosen so as to correspond to the ones used during the experiments in ref. 14. These values were chosen because the sole aim of the present investigations was to help us understand the character of the current observed in ref. 14 at low anode potentials which fall into the so-called "immune" region of Pt. As said before, it was suggested that the above currents are due also to anodic dissolution of Pt during the CMR, although the potentials at which these currents are observed fall in a region where non-renewed Pt cannot be dissolved. To clarify the above point, which is of principal importance, it was enough just to register, with sufficient reliability (which the method of Piercy and Ryan [17,18] ensures), the appearance of Pt ions at some potentials in that region, leaving for the future detailed investigations of the phenomenon — e.g. the potential dependence of the amount of Pt ions and of the current efficiency, the temperature dependence, etc. It will be necessary to carry out such further investigations because the present findings raise many further questions — for instance, what the reasons are for the observed low current efficiency of about 10%. For now, however, even the mere coloration of the solution obtained as described above allows us to draw the important conclusion with a large degree of certainty that anodic dissolution of Pt during CMR of its surface can really take place in the "immune" potential region.

The above observations can be explained in the following way. Pourbaix diagrams are constructed on the basis of data for equilibrium states of the noble metal

(non-renewed) and in its equilibrium state Pt is thermodynamically stable. It cannot be dissolved spontaneously because its thermodynamic potential is lower than the thermodynamic potential of its ions.

In the present experiments the state of the Pt (the initial state of the system for the process of dissolution) is the one which we create and maintain artificially through CMR of the oxide layer (or the layer of adsorbed oxygen). This stationary state of Pt partially or entirely cleaned from its oxide (oxygen) is irreversible and the fact that, from this state, Pt passes spontaneously into its reversible state, in which it is covered with an oxide layer, shows that through the CMR we obtained Pt of a higher thermodynamic potential (Gibbs energy) than in its reversible state. Should the potential of the cleaned Pt become higher than the thermodynamic potential of Pt ions, the spontaneous anodic dissolution of Pt becomes possible.

REFERENCES

1 Margulis, Wied. Ann., 65 (1898) 629.
2 J. Tafel and B. Emmert, Z. Phys. Chem., 52 (1905) 349.
3 S. Gilman, Electrochim. Acta, 9 (1964) 1025.
4 A.N. Chemodanov, Ya.M. Kolotyrkin, M.A. Dembrovskii and T.V. Kudryavina, Dokl. Akad. Nauk SSSR, 171 (1966) 1384.
5 P. Malachesky, R. Jasinski and B. Burrows, J. Electrochem. Soc., 114 (1967) 1104.
6 E.I. Kruscheva, M.P. Tarasevich, N.A. Shumilova and N.I. Urisson, Zashch. Met., 15 (1979) 560.
7 D.C. Johnson, D.T. Napp and S. Bruckenstein, Electrochim. Acta, 15 (1970) 1493.
8 D.A.J. Rand and R. Woods, J. Electroanal. Chem., 35 (1972) 209.
9 Yu.M. Mironov, A.N. Chemodanov, Ya.M. Kolotyrkin, G.S. Raskin, N.S. Gorbacheva and N.A. Lyubimova, Zashch. Met., 12 (1976) 532.
10 S.Ya. Vasina, O.A. Petrii and V.A. Safonov, Elektrokhimiya, 17 (1981) 270.
11 G.M. Tagirov, I.I. Ashteulova, A.N. Chemodanov and Ya.M. Kolotyrkin, Elektrokhimiya, 17 (1981) 1103.
12 L.P. Vishnyakova, Yu.L. Golin, N.M. Danchenko, Yu.S. Usmanova and O.V. Chumakovskii, Elektrokhimiya, 14 (1978) 582.
13 V.C. Noninski, Dissertation HCIT (Sofia), 1982.
14 C.I. Noninski and V.C. Noninski, J. Electroanal. Chem., 131 (1982) 355.
15 C.I. Noninski and V.C. Noninski, 32nd ISE meeting, Dubrovnik, Yugoslavia, 1981, Ext. Abstr., Vol. 1, p. 181.
16 C.I. Noninski, Khim. Ind. (Sofia), 37 (1966) 442.
17 F. Piercy and D. Ryan, Can. J. Chem., 41 (1963) 667.
18 P. Mosheva and R. Borissova, C. R. Acad. Bulg. Sci., 35 (1982) 1085.
19 M. Pourbaix, Atlas d'Equilibres Electrochimiques, Paris, 279–383.

Hydrogen evolution on freshly generated chromium electrode surfaces

V. C. NONINSKI

The effect of continuous mechanical renewal (CMR) of a chromium electrode surface on the rate of hydrogen evolution has been investigated. The increase in steady state hydrogen evolution rate at a given potential due to CMR was found not to persist after CMR had ceased.

Manuscript received 11 April 1989; in final form 18 September 1990. *The author is in the Laboratory for Electrochemistry of Renewed Electrode–Solution Interfaces (LEPGER), PO Box 9, Sofia 1504, Bulgaria.*

INTRODUCTION

The fact that a decrease in hydrogen evolution overpotential (increase of hydrogen evolution rate) occurs during continuous mechanical renewal (CMR) of the surfaces of metals with low hydrogen evolution overpotentials has been established by Tomashov *et al.*[1-3] For metals with high hydrogen overpotentials, a decrease in this overpotential (increase in the reaction rate) and in the activation energy for hydrogen evolution during CMR occurs, as has been established by C. I. Noninski and co-workers.[4-6]

A study with the aim of determining whether the increase in hydrogen evolution rate brought about by CMR of the entire electrode surface (at a given cathodic potential) persists after renewal has been stopped is reported in the present paper. This phenomenon has been investigated[7,8] by scratching a small portion of a chromium electrode to generate fresh metal discontinuously at the surface. Large increases in hydrogen evolution rate were observed on chromium at low electrode potentials in aqueous solutions when the metal surface was freshly regenerated. This reaction was observed to continue at a rapid rate long (even indefinitely) after the fresh metal surface had been created, provided the potential remained low, an effect attributed to the formation, following scratching, of an oxide film differing in properties from the original.[7,8] Further, a decay in the cathodic current occurred, which was explained on the basis of partial reformation of an oxide film and growth of hydrogen bubbles hindering mass transfer to the scratched surface.

EXPERIMENTAL METHOD

The fresh metal surface was created by a selfcleaning rotating electrode (SRE), described in detail elsewhere.[6,9,10] Renewal of the electrode (99·9%Cr, surface area ~5 mm^2) occurs when the cone shaped working electrode, which is pressed on the four sharp edges of the sharpener (made of baked corundum), is rotated at 50 Hz. The special construction of the sharpener makes it possible to renew the entire surface of the SRE continuously at a controlled rate with practically no screening effect. Thus, a SRE allows steady state processes occurring on a continuously generated fresh metal surface to be compared with those on a non-renewed surface, i.e. when the cone surface is not being rotated. The reproducibility of results obtained during CMR is very high[11-13] – much higher than in its absence – and depends strongly on the preparation of the SRE. Because of the extended periods involved in the present experiments, it was not possible to use one electrode throughout and although the results for a given electrode are highly reproducible, the data obtained with different electrodes under the same conditions will differ slightly due to intrinsic differences. However, these variations are not significant in the context of the present investigation.

The experiments were carried out in a standard three compartment glass cell similar to that described previously.[10] Water traps, with which both the cell and the SRE were fitted, made it possible to isolate the working compartment from the atmosphere. A saturated calomel electrode was used as the reference electrode with a Luggin capillary situated <1 mm from the electrode surface, thus making any Ohmic correction of the potential virtually unnecessary. The counter electrode consisted of a platinum gauze and the anode and cathode compartments were separated by a porous membrane. The solution was saturated with argon (99·995% pure) throughout the experiment and the temperature of the cell was maintained constant at 293 ± 1 K. The working electrolyte was analytical grade 1M KOH prepared with doubly distilled water. Polarisation was controlled with a potentiostat–galvanostat Radelkis OH–405 (Hungary) and the transients recorded on an x–y recorder 620.02 (GDR).

Transients consisting of three main regions – before, during, and after CMR – were generated while a cathodic potential was applied to the electrode. However, there is a further factor that should also be considered. The electrodes were exposed to the atmosphere, usually overnight, before use, during which time oxide layer(s) were formed on the surface. While the use of a SRE makes it possible to remove this oxide from the electrode surface, so allowing measurements to be made on a virtually oxide free surface, it should be noted that several hundred rotations of the electrode are required to achieve this condition. It was therefore possible to obtain two types of transient:

(i) from electrodes having surface oxide layers, i.e. after exposure to air overnight
(ii) from electrodes that had been mechanically cleaned (while immersed in the test solution) to remove oxide layers immediately before applying the potential and commencing measurement.

RESULTS AND DISCUSSION

The transient from an experiment of type (i) is presented in Fig. 1*a*; the applied potential was −1·300 V(NHE). It can be seen that in the first few tens of seconds after application of the potential a characteristic minimum is observed in the current–time transient, after which the current increases gradually until reaching state A. Mechanical removal of the electrode surface was commenced 1060 s after application of the potential, whereupon the current increased suddenly to a maximum, then began gradually to decrease. After about a further 880 s CMR was ceased, producing a sudden drop in the current followed by a period of slower decrease. About 980 s after ceasing CMR state B was established. The reaction rate in state B is lower than that in state A.

It might appear that this result answers the question raised initially. However, it was found that if the chro-

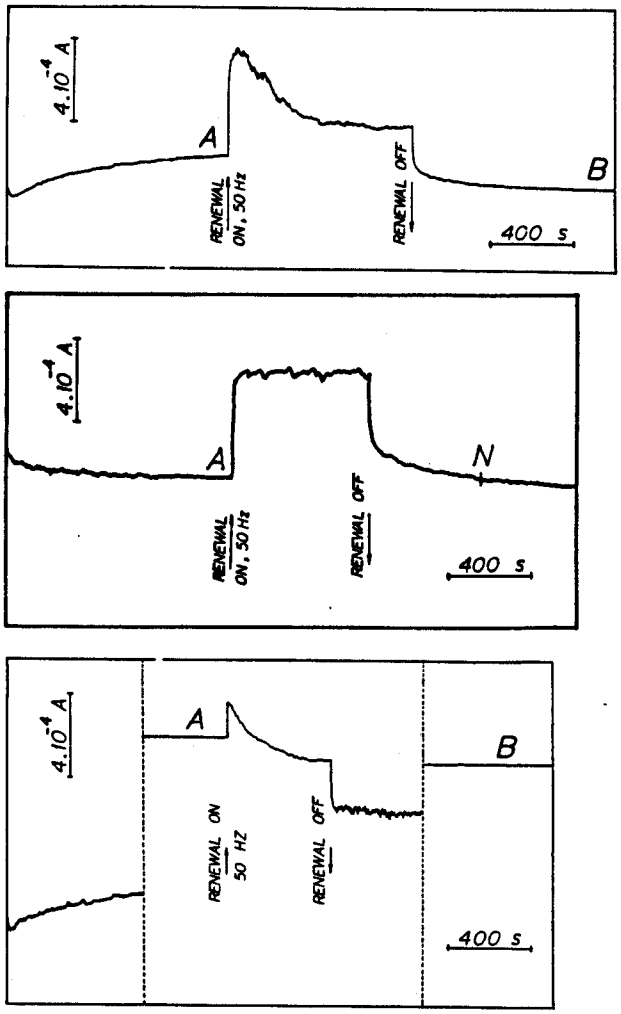

a electrode kept overnight in air at ambient temperature: *b* different electrode from *a* with surface mechanically renewed immediately before start of measurement; *c* same electrode as in *b* after exposure overnight in air at ambient temperature: broken lines indicate 20 h break in recording

1 *Cathodic current transients recorded during hydrogen evolution on chromium selfcleaning rotating electrode held at −1·300 V(NHE) in 1M KOH solution: start of curve represents application of potential; ↑ marks start and ↓ cessation of continuous mechanical surface renewal*

mium electrode surface was renewed just before starting type (ii) experiments, effects contrary to those shown in Fig. 1*a* could be observed (Fig. 1*b*). In this test the chromium surface was renewed in the solution for several minutes, after which CMR was stopped and the curve shown in Fig. 1*b* recorded. At least two types of phenomena relevant to the aims of the present study can be seen, at different stages on the curve. The current in state A of Fig. 1*b* (corresponding to state A in Fig. 1*a*) is lower than that at point N (after stopping CMR, but still maintaining the applied potential). Here, and especially in the region before N where the currents are markedly different, it would be reasonable to conclude, similarly to Burstein *et al.*[8] and C. I. Noninski,[9] that the effect of CMR *is* preserved after the process ceases.

However, at point N in Fig. 1*b* (530 s after ceasing CMR), the current is equal to that in state A. Thus, if currents are compared after point N, i.e. more than 530 s from ceasing CMR, the conclusion will be the same as that drawn from Fig. 1*a*: namely, that the effect of renewal is *not* preserved after the process is stopped.

The main reason for this apparent ambiguity lies in the fact that comparison is in some cases being made between non-steady state currents. Such non-steady state comparisons appear to have been applied by Burstein *et al.*[7,8] The transients presented in Fig. 1 of both these papers were recorded for the relatively short time of ~6 s (in Fig. 2 of Ref. 7 this period is 7 s) after cessation of scratching. In Fig. 1 of Ref. 8 a steady state regime appears to have been established several seconds after scratching is stopped, although it is relevant to note that this figure has an enlarged abscissa scale which could affect this judgement. The lowest rate of change on this figure appears to be of the order of 1 mA h^{-1}, which can reasonably be represented as a measureable value that is not indicative of steady state conditions. Thus, the claims of Burstein *et al.*[8] discussed above could be regarded as precipitate.

In an attempt to resolve the apparent ambiguity, experiments were carried out for periods sufficient to ensure that current would remain unchanged for several hours (within the limits of accuracy of the measuring system). In the present case steady state conditions were considered to have been achieved when the rate of change became <0·01 mA h^{-1}.

In Fig. 1*c* cathodic current is shown as a function of time in a type (i) experiment. It can be seen that the curve has a characteristic initial form, which, in the course of time, tends toward higher current values. This tendency was persistent and it was only after ~2 h that the rate of increase became <0·01 mA h^{-1} (A in Fig. 1*c*). After establishing a steady state current, CMR was carried out for several minutes, sufficient for the entire cathodic surface to have been renewed. This resulted (Fig. 1*c*) in a rapid increase in current to a maximum, after which a decrease to a steady state value was observed. The current recorded in Fig. 1*c* just before CMR was ceased had remained constant over a period of many hours (this is not shown in the figure for clarity) at a level that was lower than the steady state current obtained in the absence of CMR. After ceasing renewal, the current rapidly decreased to a level significantly lower than the steady state value in the absence of renewal. (Although it would appear from Fig. 1*c* that the current has reached a steady state value several minutes after stopping CMR, this value is in fact reached only after ~20 h – state B.)

It can be seen from Fig. 1*c* that the current in state B (the steady state reached after stopping CMR, but maintaining the applied potential) is lower than that in state A (steady state before CMR). This is observed not only at −1·300 V(NHE), but also at other potentials within the Tafel region when the initial condition of the chromium electrode is similar and is a difference arrived at as a result of comparing steady state currents, unlike in Fig. 1*a* and *b* where comparison of non-steady state conditions is being made. The steady state current density recorded on the filmed surface is an order of magnitude greater than that given in Ref. 8 for unscratched chromium, whereas the steady state current densities for both filmed and unfilmed chromium surfaces in Fig. 1*c* are of the same order of magnitude as the steady state scratch current density given in Ref. 8.

The increase in current during cathode polarisation of non-renewed chromium can be attributed to an increase in activity due to the decrease in thickness of the surface oxide film brought about by cathodic reduction of the latter. Differences in the processing history of the chromium electrodes (not controlled here or in Refs. 7 and 8) can lead to electrodes used in different experiments having dissimilar initial oxide thicknesses, which will affect the time necessary to achieve steady state conditions. Nevertheless, the qualitative conclusions drawn from the separate experiments should still be valid.

During CMR of the electrode surface it is probable that not only the rate of hydrogen evolution but also that of refilming is increased. Because of CMR, refilming is not

rapid enough and hydrogen evolution takes place on an activated surface. The form of the curve recorded during CMR reflects the fact that the surface state of the electrode is changed to a greater extent during CMR than is that of a non-renewed electrode because of increased catalytic activity of the electrode surface towards water molecules. It should be noted also that steady state conditions are reached several orders of magnitude faster during CMR of the electrode surface.

In considering these results it should be emphasised that several hundred rotations of the electrode are necessary for the renewal of the entire surface. This would explain the observed difference in the initial form of curves obtained during CMR for the same electrode (Fig. 1*b* and *c*), although the steady state currents during CMR practically coincide. As discussed above, the value of the steady state current is determined by competition between the processes of activation and refilming. The initial form of the curves during CMR in Fig. 1*b* and *c*, however, is determined by the processing history of the electrode. In Fig. 1*b* the CMR necessary to renew the entire surface has been applied before commencing measurement (type (ii) experiment) and no stable oxide layer has been able to form in the initial period when potential is applied without CMR. Therefore, on commencing CMR a steady state is reached rapidly – the current has a practically constant value from the very beginning of renewal.

Similarly, in the case shown in Fig. 1*c* the electrode surface was cathodically reduced for ~20 h and has reached a steady state in the absence of CMR. When CMR is applied the competing processes already mentioned eventually produce a steady state current practically coinciding, as expected, with that during CMR in Fig. 1*b*, but lower than that for the prior oxide covered chromium.

After CMR is stopped, refilming continues unopposed, as a result of which the rate of hydrogen evolution is decreased.

CONCLUSIONS

The effect of continuous mechanical renewal of the entire surfaces of chromium electrodes held at −1·300 V(NHE) in 1M KOH solution was investigated. It has been established that the steady state evolution rate of hydrogen obtained under such conditions does not persist after renewal has been stopped, even when polarisation is maintained.

REFERENCES

1. N. D. TOMASHOV, N. M. STRUKOV, and L. P. VERSHININA: *Dokl. Akad. Nauk SSSR*, 1966, **171**, 1134.
2. N. D. TOMASHOV and L. P. VERSHININA: *Electrochim. Acta*, 1970, **15**, 501.
3. N. D. TOMASHOV, N. M. STRUKOV, and L. P. VERSHININA: *Elektrokhimia*, 1969, **5**, 26.
4. C. I. NONINSKI: *Khim. Ind.*, 1972, **44**, (3), 121.
5. C. I. NONINSKI and I. P. IVANOV: *Khim. Ind.*, 1975, **47**, (2), 70.
6. C. I. NONINSKI: *Bull. Soc. Chim.*, 1976, (9–10), 1283.
7. G. T. BURSTEIN and M. A. KEARNS: *J. Electrochem. Soc.*, 1984, **131**, 991.
8. G. T. BURSTEIN, M. A. KEARNS, and J. WOODWARD: *Nature*, 1983, **301**, 692.
9. C. I. NONINSKI: *Khim. Ind.*, 1966, **37**, 442.
10. C. I. NONINSKI and V. C. NONINSKI: *J. Electroanal. Chem.*, 1982, **131**, 355.
11. V. C. NONINSKI and E. B. SOBOWALE: *Sci. Pharm.*, 1986, **54**, 105.
12. V. C. NONINSKI and E. B. SOBOWALE: *Coll. Czech. Chem. Commun.*, 1987, **52**, 66.
13. V. C. NONINSKI and E. B. SOBOWALE: *Farmacia*, 1987, **35**, 175.

EXCESS HEAT DURING THE ELECTROLYSIS OF A LIGHT WATER SOLUTION OF K_2CO_3 WITH A NICKEL CATHODE

COLD FUSION

TECHNICAL NOTE

KEYWORDS: *excess energy, electrolysis of H_2O, nickel cathode*

V. C. NONINSKI* *Laboratory for Electrochemistry of Renewed Electrode-Solution Interface (LEPGER), P.O. Box 9, Sofia 1504, Bulgaria*

Received July 5, 1991
Accepted for Publication August 19, 1991

Experimental results of differential heat loss calorimetry measurements during the electrolysis of light water solutions of K_2CO_3 and Na_2CO_3 with a nickel cathode are presented. A significant increase in temperature with every watt input, compared with the calibration experiment, is observed during the electrolysis of K_2CO_3. This effect is not observed when Na_2CO_3 is electrolyzed. No trivial explanation (in terms of chemical reactions, change in heat transfer properties, etc.) of this effect has been found so far. If the nontriviality of the observed overcoming of the energy breakeven barrier is further confirmed, this phenomenon may find application as an important new energy source.

INTRODUCTION

The studies in this paper follow the general lines of the work of Fleischmann and Pons,[1] although electrolysis of D_2O is usually considered when excess energy is claimed. Observation of excess energy production during the electrolysis of H_2O was first mentioned by Pons and later rejected.[1] Pons et al., however, explicitly state the possibility of obtaining excess energy during electrolysis of ordinary water (using nickel as a cathode, among other proposed metals) in Ref. 2. Unexplained excess heat in light water is also claimed in a paper by Bush et al.[3] Mills and Kneizys[4] claim to have obtained excess energy above the amount spent during the electrolysis of a K_2CO_3 ordinary water solution with a nickel cathode. The excess energy effect, according to these authors, is not observed when Na_2CO_3 is electrolyzed. Furthermore, unusual effects during the electrolysis of light water have also been reported by Matsumoto.[5]

This paper compares the heating coefficients for a nickel/platinum (Ni/Pt) circuit with those for a resistor heater in vacuum-jacketed dewar electrolytic cells containing K_2CO_3 or Na_2CO_3. Note that the excess energy effect from an electrochemical system containing K^+ (Li^+ is usually used in these studies) in D_2O is reported in Ref. 6.

*Visiting scholar at Franklin and Marshall College, Chemistry Department, Lancaster, Pennsylvania.

EXPERIMENTAL DETAILS

The experiments were carried out by observing and comparing the temperature difference, $\Delta T_1 = T_{electrolysis\ only} - T_{blank}$ and $\Delta T_2 = T_{resistor\ heating\ only} - T_{blank}$ referred to unit input power, between two identical 200-ml silver-coated vacuum-jacketed dewars. A calorimeter dewar having the same configuration and containing the same amount of electrolyte, same type of electrodes (nickel cathode and platinum anode), resistor heater, and thermistor (thermometer) and stirred at the same speed was used as a blank; neither electrolysis nor heating by the resistor was carried out in this dewar. Experiments were also carried out by using as a blank a dewar used in a previous experiment and vice versa. This exchange was done to ensure that the effect was not due to any difference in the thermal properties of the two specific dewars used. Each dewar had a 3-cm opening, and a 2-cm-thick tapered rubber stopper was placed 1 cm into the dewar. The experimental apparatus for the differential calorimetry used in these studies is shown in Fig. 1. Unlike the studies in Ref. 4, the resistor and the electrolytic circuit were not run simultaneously in this study; the effects of heating by the resistor and by the electrolysis circuit were studied in separate runs.

As is usual in electrochemistry, measures were taken to avoid impurities in the system, especially organic substances. While it is unclear at this point what the relationship is, if any, between the contamination effect on the hydrogen overpotential and that on the eventual excess heat, one should recall the known problems with the reproducibility of the hydrogen overpotential, which can be overcome only by ensuring the lowest possible level of impurities. Certain procedures should be applied to reproduce the excess heat effect. For instance, before starting the experiment, mechanically scour the platinum anode with steel wool, soak overnight in concentrated HNO_3, and then rinse with distilled water. Remove the nickel cathode from its container with rubber gloves, and cut and bend it in such a way such that no organic substances are transferred to the nickel surface. Preferably, dip the nickel cathode into the working solution under an electrolysis current, and avoid leaving the nickel cathode in the working solution in the absence of an electrolysis current. Clean the electrolysis dewar, and free it of organic contaminants.

After assembling the experimental setup, the nickel cathode was subjected to anodizing by a constant electrolysis current of 0.083 A for 1 h. Then, the direction of the electrolysis

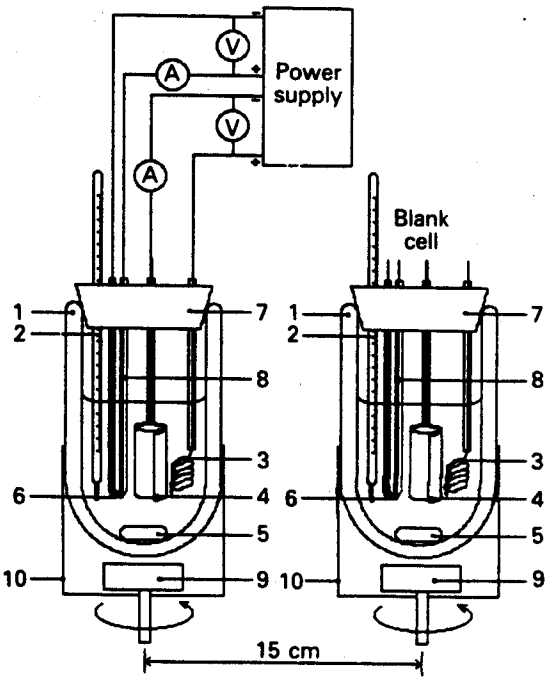

Fig. 1. Experimental setup: (1) vacuum-jacketed dewar, (2) thermometer, (3) platinum anode, (4) nickel cathode, (5) magnetic stirring bar, (6) resistor heater, (7) rubber stopper, (8) Teflon tubing, (9) magnetic stirrer, and (10) aluminum cylinder.

current was reversed (platinum anode and nickel cathode), and the electrolysis was carried out for 14 to 16 h.

The electrolysis heating power was calculated as $P_{el} = (E_{el} - 1.48)I_{el}$, where E_{el} is the applied electrolysis voltage, I_{el} is the electrolysis current (the term "electrolysis power" is used here for convenience, denoting only the power contributing to the joule heating effect during the electrolysis), and 1.48 V is the isoenthalpic voltage, which at the temperatures studied practically coincides with the thermoneutral voltage. The resistor heater power was calculated as $P_h = I_R E_R$, where I_R denotes the resistor current and E_R denotes the resistor voltage.

The cathode was a 7.5-cm-long × 4-cm-wide × 0.0125-cm-thick nickel foil (Aldrich 99.9+%) spiralled into a cylindrical form. The anode was a 0.1-cm-diam × 10-cm-long platinum wire (Johnson-Matthey). The spiral anode and the cylindrical cathode were parallel to each other. The leads were inserted into Teflon tubes to prevent any recombination of the evolving gases. The electrolyte solution in both dewars was 153 ml of 0.57 M K_2CO_3 or 0.57 M Na_2CO_3 in H_2O. The distilled water was from the common distiller of the Chemistry Department of Franklin and Marshall College. The power was delivered by a Zenith SP-2718 power supply (alternating current component <0.1%). The resistance heater was a 100-Ω, 1% precision, metal oxide resistor in a 2-mm-o.d. Teflon tube. The electrolyte solution in both dewars was stirred simultaneously (synchronized for the two dewars) by two identical spheroidal ellipse magnetic bars rotated by two magnetic stirrers at ~300 rpm. Electrolysis voltage and current were measured by two Keithley 169 multimeters, and the resistor voltage and current were measured by Extech 380198 and Micronta 22-185 A multimeters with 0.01-V and 0.001-A accuracy, respectively. The use of vacuum-jacketed dewars, rather than air-jacketed dewars or simple flasks, made the measurements more sensitive (higher heating coefficient). In a vacuum-jacketed dewar unit, input power leads to a greater steady-state temperature, thus enabling differences in steady-state temperatures (for the same configuration) to be more pronounced. The temperatures in this study were monitored continuously using the capability of the standard calorimeters (Parr P-318) to record the temperature continuously (with 0.01°C accuracy) on their strip-chart recorder (Fisher Recordall Series 5000).

RESULTS AND DISCUSSION

The results of the study are shown in Figs. 2 through 5. Figure 4 is based on the data presented in Figs. 2 and 3. Figure 2 shows the absolute change in the measured temperatures of the dewars at different conditions, while Fig. 3 shows the input powers in each case. It can be seen from Fig. 3 that while the input power with the resistors working was constant as expected, the input electrolysis power was not, and there is a time lag between the application of power and the temperature response. We compensated for this by selecting appropriate power values when calculating the heating coefficients plotted in Fig. 4 (more precisely, the term "heating coefficient" refers only to the steady-state values of the quantities in Fig. 4; the last parts of the curves in Fig. 4 can be considered to represent steady state). The heating coefficients plotted in Fig. 4 were calculated using the average power plotted in Fig. 3. Note that other reasonable ways of referring the observed ΔT to the applied power are possible; however, even the most conservative approach gives the same qualitative effect as that seen in Fig. 4. Studies currently in progress, using a data acquisition system, show sustained steady-state production of excess heat for many days. Results from these studies are presented elsewhere.

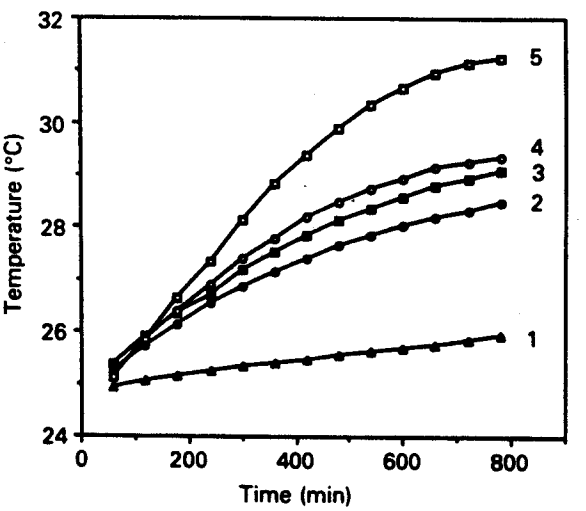

Fig. 2. Time history of temperatures: (1) blank cell (this curve is used as the blank for computing the heating coefficients of Fig. 4); (2) K_2CO_3 calibration cell (with only resistor heater working); (3) Na_2CO_3 calibration cell; (4) K_2CO_3 electrolysis cell (with only electrolysis working); and (5) Na_2CO_3 electrolysis cell.

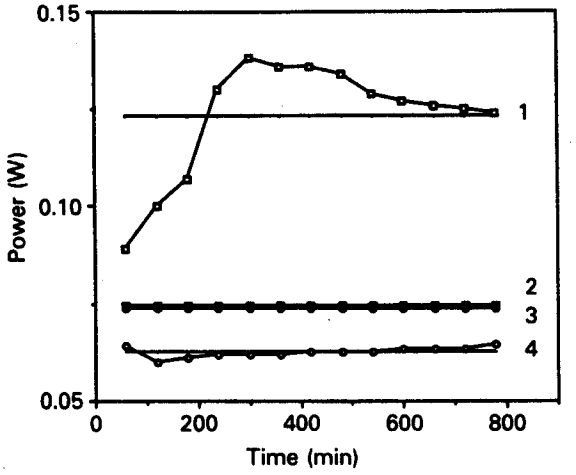

Fig. 3. Time history of the applied power: heating power with (1) electrolysis in the Na_2CO_3 cell, (2) the resistor in the Na_2CO_3 cell, (3) the resistor in the K_2CO_3 cell, and (4) electrolysis of the K_2CO_3 cell. The thermoneutral voltage is 1.48 V. For the calculations presented in this paper, mean values of the electrolysis powers in the Na_2CO_3 and K_2CO_3 cells are used, shown as solid lines in curves 1 and 4.

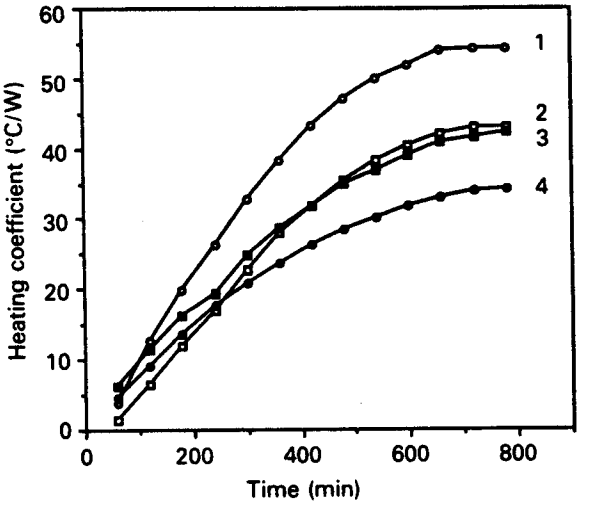

Fig. 4. Plot of the heating coefficients over time: (1) electrolysis at 0.083 A in K_2CO_3, (2) resistor working in Na_2CO_3, (3) electrolysis at 0.083 A in Na_2CO_3, and (4) resistor working in K_2CO_3.

The heating coefficient of the Na_2CO_3 cell is plotted in Fig. 4. The heating coefficient for the resistor heater only and that for the electrolysis circuit only are essentially identical. This is to be expected for a given dewar and a given electrolyte when steady state is reached: The ΔT corresponding to a unit heating power has a strictly defined value, determined by the properties of the materials through which heat is being lost. The properties of the cell are unaltered during operation. Specifically, the volume of electrolyte remains practically constant: ~0.2% of the solution volume is being electrolyzed during the 12-h operation of the Ni/Pt cell.

In contrast, the calorimeter containing K_2CO_3 showed very different behavior. The heating coefficient of the K_2CO_3 cell is plotted over time in Fig. 4. The heating coefficient-time curve of the working electrolysis cell is clearly above the curve of the dewar in which only a resistor is working. The value of the heating coefficient with the Ni/Pt circuit working is ~50°C/W, while the heating coefficient with only the resistor working is ~30°C/W. Therefore, the output power obtained through the Ni/Pt circuit is ~160% of the input power. The time-integrated power (i.e., energy) input into the system during the course of the experiment in Fig. 4 is ~4800 J compared with the output power of ~8000 J. Thus, Fig. 4 shows a significant difference in the thermal behavior of two identical systems that differ only in the positive ions of the salt.

A trivial explanation for this behavior of the K_2CO_3 cell is not straightforward. In fact, the electrolysis should be expected to lead to a decrease in the heating coefficients compared with those of the cells in which only the resistor is working ". . . consistent with additional heat losses caused by gas evolution . . . ,"[7] which is currently observed only in the Na_2CO_3 cell.

The erroneous attribution of the effect to temperature gradients was eliminated by testing for minute spatial variations of the temperature over time. Three thermistors were positioned ~2.5 cm apart at the bottom, middle, and upper part of the electrolyte. The results, shown in Fig. 5, clearly demonstrate that no difference is observed (within the limit of detection, 0.01°C).

Note that the electrolysis is always started with a newly manufactured cathode from the batch of 99.9%+ purity nickel. The use of new nickel excludes any possibility that the effect is due to the decomposition of species formed before the beginning of the electrolysis. The reaction of hydride formation is exothermic with a standard enthalpy of formation[8] of -8.79 ± 0.59 kJ·mol^{-1} H_2. However, if all of the hydrogen evolved during the run became hydride, an energy contribution would result that is more than one order of magnitude less than the excess heat that is observed according to Fig. 4. This can easily be calculated based on the amount of hydrogen evolved over ~12 to 14 h at a rate of 0.083 A. Although the overall amount of energy produced in the experiment is relatively low, it is clear that the observed effect is outside the error limit of the experiment, which is of the order of ±1°C/W, calculated from the accuracies of the measured parameters at the respective ranges.

It is not known what trivial chemical reaction might be triggered by the applied electrolysis that would be capable of producing the observed amount of excess heat. Some exotic farfetched possibilities for explaining the difference in electrochemical behavior between K_2CO_3 and Na_2CO_3 can be postulated. One such example is the formation of formic acid, e.g., by the reaction $HCO_3^- + 2H_2O \rightarrow HCOOH + 3OH^-$, or methane if $KHCO_3$ is present in the electrolyte. However, even if such possibilities are invoked, it should not be forgotten that energy is also being spent for these electrochemical reactions, which will again result in an isoenthalpic (or thermoneutral) voltage. In most cases, the value of this thermoneutral voltage may exceed 1.48 V, which will cause cooling rather than heating of the solution. This is indicative of even higher excess energy values. A reaction that readily comes to mind is oxygen reduction. It is well known, however, that nickel is a poor catalyst of oxygen reduction, and the current density of this reaction is negligibly small compared with the current density applied here (~1 mA/cm^2).

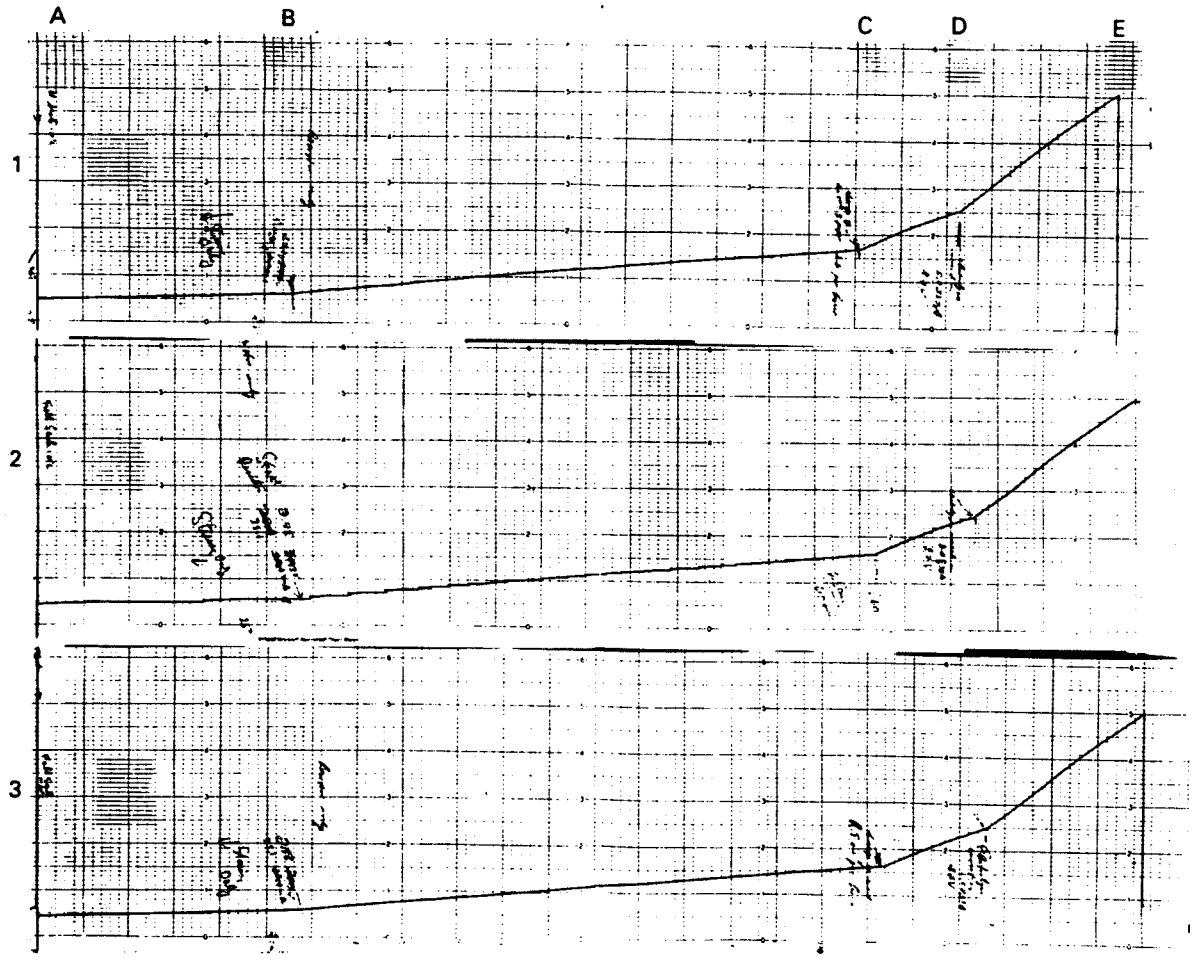

Fig. 5. Temperature changes at three points within the solution: (1) at the top, (2) in the middle, and (3) at the bottom. The setup used for this study is similar to that presented in Fig. 1, but in the working cell there are three thermistors instead of one. Section A-B: x axis scale = 30 division/h, y axis scale = 0.2°C/division, stirring only; section B-C: x axis scale = 30 division/h, y axis scale = 0.2°C/division, resistor only; section C-D: x axis scale = 5 division/h, y axis scale = 0.2°C/division, resistor only; and section D-E: x axis scale = 5 division/h, y axis scale = 0.2°C/division, electrolysis only.

These possibilities were rejected after study of the correspondence of the Faraday efficiency of the evolved H_2 and O_2 gases. This was done in a separate experiment by collecting the evolved gases and comparing the measured volume of the gases with the volume corresponding to the quantity of electricity that had passed through the cell over a given time. Note also that the absence of appreciable $H_2(D_2) + O_2$ recombination has been noted by a number of investigators, even in systems that contain metals (e.g., palladium) that are known to be good catalysts of that reaction (e.g., Refs. 9 through 14). Other preliminary studies (mass spectroscopy, pH measurements, titration) before and after the experiment showed no unexpected species or pH change. These studies should be continued further.

The problem of recombination is a crucial one in this study (note again that the excess heat here is calculated after subtracting 1.48 V), however, and it deserves special attention in any further experiments. On the other hand, as we have noted,[6] the problem of recombination (and the other connected calorimetric problems) preferably should not be solved by studying the effect in a closed cell with a recombiner. The recombiner adds new unknowns since the kinetics of the recombination of H_2 and O_2 to H_2O should be well understood through studies such as those in Ref. 15. On the other hand, since the claimed excess energy itself is a newly found, unstudied phenomenon, no additional conditions should be imposed because their eventual effect on the reproducibility of the excess energy is unknown. For instance, it is not clear whether the ability of the recombiner to recombine not only the H_2 and O_2 evolving through electrolysis but also all other quantities of H_2 and O_2 existing in the gas and the liquid phase, thus creating concentration gradients, will be a hindering factor for the appearance of excess energy.

An explanation for the increase in the heating coefficient for a Ni/Pt circuit might be that an additional source of energy of unknown nature is acting from within that adds to the energy input to the cell from without. If this nontrivial possibility is confirmed, this effect will be of great importance as an alternative energy source. Further calorimetric sophistication is necessary to further confirm the reality of the observed effect and to obtain a quantitative assessment of its magnitude. For instance, to avoid errors of a subjective nature, a data acquisition and processing system is necessary. The measurements should be carried out at constant input

power and for longer periods of time so that curves like curve 1 of Fig. 2 reach a clear and sustained steady state. Maintaining a constant ambient temperature is also a requirement in these studies. Such studies are now in progress. To fully avoid concerns connected with the peculiarities of heat transfer during bubble evolution, it is necessary, together with heat loss calorimetry measurements (including Seebeck), that this effect be observed in an adiabatic-type calorimeter (bomb calorimeter) similar to the one used in Ref. 6. Note, however, that despite the opinions of some researchers, if careful studies are carried out, calorimetric techniques are not only capable but are the only ones that can decisively prove (or disprove) the reality of the effect in question. There is also no reason to expect that time spans of tens of hours will be insufficient to definitely rule out (or conclusively confirm) a trivial explanation of the observed effect if the studies are conducted carefully. It seems, however, that the reality of the effect can qualitatively be established with the described procedure. It seems also that the reported effect is reproducible and can easily be demonstrated.

It is the author's understanding that speculations (invoking reactions of nuclear or any other origin) as to why overcoming the energy breakeven barrier might come about should be carried out only after firmly establishing the reality of the claimed effect through experiments. This circumstance is not new for science. One may recall the experimental findings of Davison and Germer, Einstein, Wien, Compton, and others, which were unexplainable at the level of knowledge at their time. These experimental findings virtually caused the birth of 20th century physics, especially quantum mechanics. Even one of the most recent scientific discoveries—high-temperature superconductivity—whose reality is undeniable, still remains unexplained, which does not make this experimentally found effect less important.

Since the problem of the reality (nontriviality) of the excess energy reported here is of primary concern, we leave open the questions for the theoretical explanation of the phenomenon.

CONCLUSIONS

The experimental results presented here show that there is more evidence than usually considered for the eventual production of excess energy during the electrolysis of water. Therefore, further efforts seem to be justified for verifying the claim of Fleischmann and Pons for overcoming the energy breakeven barrier through electrolysis.

Contrary to the opinion expressed in Refs. 16 and 17, it does not seem plausible that light water should be used as a "control" when excess energy is being sought during the electrolysis of heavy water.

ACKNOWLEDGMENTS

The author wishes to thank J. J. Farrell, Franklin and Marshall College, for his kind invitation to use his laboratory for these studies. Thanks are also due to James McBreen, Brookhaven National Laboratory; David Worledge, Electric Power Research Institute; and M. H. Miles, Naval Weapons Center, for useful discussions. The author would like to thank also W. R. Good for technical help.

The author also wishes to thank the two referees for their careful reading of the manuscript and for their useful remarks.

REFERENCES

1. M. FLEISCHMANN and S. PONS, "Electrochemically Induced Nuclear Fusion of Deuterium," *J. Electroanal. Chem.*, **262**, 301 (1989); see also Errata, *J. Electroanal. Chem.*, **263**, 187 (1989).

2. S. PONS, M. FLEISCHMANN, C. WALLING, and J. SIMONS, "Method and Apparatus for Power Generation," International Application Published Under Patent Cooperation Treaty (PCT/US90/01328; International Publication Number WO 90/10935) (Mar. 13, 1989).

3. B. F. BUSH, J. J. LAGOWSKI, M. H. MILES, and G. S. OSTROM, "Helium Peoduction During the Electrolysis of D_2O in Cold Fusion Experiments," *J. Electroanal. Chem.*, **304**, 271 (1991).

4. R. L. MILLS and S. P. KNEIZYS, "Excess Heat Production by the Electrolysis of an Aqueous Potassium Carbonate Electrolyte and the Implications for Cold Fusion," *Fusion Technol.*, **20**, 65 (1991).

5. T. MATSUMOTO, "Cold Fusion Observed with Ordinary Water," *Fusion Technol.*, **17**, 490 (1990).

6. V. C. NONINSKI and C. I. NONINSKI, "Determination of the Excess Energy Obtained During the Electrolysis of Heavy Water," *Fusion Technol.*, **19**, 364 (1991).

7. G. M. MISKELLY, M. J. HEBEN, A. KUMAR, R. M. PENNER, M. J. SAILOR, and N. S. LEWIS, "Analysis of the Published Calorimetric Evidence for Electrochemical Fusion of Deuterium in Palladium," *Science*, **246**, 793 (1989).

8. G. ALEFELD and J. VOLKL, Eds., *Hydrogen in Metals II*, p. 173, Springer-Verlag (1967).

9. V. J. CUNNANE, R. A. SCANNELL, and D. J. SCHIFFRIN, "$H_2 + O_2$ Recombination in Non-Isothermal, Non-Adiabatic Electrochemical Calorimetry of Water Electrolysis in an Undivided Cell," *J. Electroanal. Chem.*, **269**, 163 (1989).

10. R. C. KAINTHLA et al., "Sporadic Observation of the Fleischmann-Pons Heat Effect," *Electrochim. Acta*, **34**, 1315 (1989).

11. D. E. WILLIAMS et al., "Upper Bounds on 'Cold Fusion' in Electrolysis Cells," *Nature*, **342**, 375 (1989).

12. T. R. JOW, E. PLICHTA, C. WALKER, S. SLANE, and S. GILMAN, "Calorimetric Studies of Deutrated Pd Electrodes," *J. Electrochem. Soc.*, **137**, 2473 (1990).

13. D. ALBAGLI et al., "Measurement and Analysis of Neutron and Gamma-Ray Emission Rates, Other Fusion Products, and Power in Electrochemical Cells Having Pd Cathodes," *J. Fusion Energy*, **9**, 133 (1990).

14. J. DIVISEK, L. FURST, and J. BALEJ, "Energy Balance of D_2O Electrolysis with a Palladium Cathode. Part II. Experimental Results," *J. Electroanal. Chem.*, **278**, 99 (1990).

15. M. J. JONCICH and N. J. HACKERMAN, "The Reaction of Hydrogen and Oxygen on Submerged Platinum Electrode Catalysts. I. Effect of Stirring, Temperature and Electric Polarization," *J. Phys. Chem.*, **57**, 674 (1953).

16. H. FURST, cited after "Hopes for Nuclear Fusion Continue to Turn Cool," *Nature*, **338**, 691 (1989).

17. J. MADDOX, "What to Say About Cold Fusion," *Nature*, **338**, 701 (1989).